JOURNAL OF GEOPHYSICAL RESEARCH, VOL. 103, NO. C6, PAGES 12,761-12,782, JUNE 15, 1998

Estimate of bottom and surface stress during a spring-neap tide cycle by dynamical assimilation of tide gauge observations in the Chesapeake Bay

Y. H. Spitz

College of Oceanic and Atmospheric Sciences, Oregon State University, Corvallis

J. M. Klinck

Center for Coastal Physical Oceanography, Old Dominion University, Norfolk, Virginia

Abstract. Dynamical assimilation of surface elevation from tide gauges is investigated to estimate the bottom drag coefficient and surface stress as a first step in improving modeled tidal and wind-driven circulation in the Chesapeake Bay. A two-dimensional shallow water model and an adjoint variational method with a limited memory quasi-Newton optimization algorithm are used to achieve this goal. Assimilation of tide gauge observations from 10 permanent stations in the Bay and use of a two-dimensional model adequately estimate the bottom drag coefficient, wind stress, and surface elevation at the Bay mouth. Subsequent use of these estimates in the circulation model considerably improves the modeled surface elevation in the entire Bay. Assimilation of predicted tidal elevations yields a drag coefficient, defined in the hydraulic way, varying between 2.5×10^{-4} and 3.1×10^{-3}. The bottom drag coefficient displays a periodicity corresponding to the spring-neap tide cycle with a maximum value during neap tide and a minimum value during spring tide. From assimilation of actual tide gauge observations, it is found that the fortnightly modulation is altered during frontal passage. Furthermore, the response of the sea surface to the wind forcing is found to be more important in the lower Bay than in the upper Bay, where the barometric pressure effect seems to be more important.

1. Introduction

Estuarine circulation, due to the combined effects of tide action, horizontal salinity gradients, river runoff, and meteorological forcing (wind stress, inverted barometer effect), has been intensively studied in the Chesapeake Bay and its tributaries and is still an ongoing source of research activity. Diverse investigations from field observations, e.g., temperature, salinity, current, and surface elevation, and from simple models were first carried out in order to explain the gravitational and tidal circulation [*Officer*, 1976; *Fisher*, 1986]. It is only during the last two decades that wind-driven circulation has been shown to be as important as the gravitational circulation, indeed the dominant nontidal circulation at times [*Wang and Elliott*, 1978; *Wang*, 1979a, b; *Paraso and Valle-Levinson*, 1996]. While the response of the water to the wind forcing in the Bay is complex, several studies have shown that sea level fluctuations depend on local winds (local forcing) and exchange between coastal ocean and estuary (nonlocal forcing). The present study focuses on the barotropic circulation in the Chesapeake Bay, forced by oceanic tides and surface winds.

While the wind, bottom friction, and exchange between the Chesapeake Bay and the open ocean have been recognized as the main forcings for the Bay circulation, the main difficulty in tidal and wind-driven circulation modeling arises from the determination of theses forcings. Indeed, bottom friction is hard to measure. *Wright* [1989] and *Wright et al.* [1987, 1992] found that large spatial and temporal variations in the bottom roughness result in large variations in the bed shear stress and the hydraulic roughness. There is also a strong indication that the biogenic roughness dominates the flow-induced roughness in the Bay stem. In barotropic models, the bottom stress is usually parameterized as a quadratic function of the vertically integrated velocity, and an empirical parameter, the bottom drag coefficient, is often determined by fitting the modeled M_2 tidal elevation and the observations at tide gauge stations [*Crean et al.*, 1988]. In baroclinic models, the bottom stress is often computed by using closure schemes such as in work by *Mellor and Yamada* [1974], which also require defining empirical parameters.

Paper number 98JC00797.
0148-0227/98/98JC-00797$09.00

Surface stress determination is another challenge for modelers. The stress is usually parameterized as a quadratic function of the wind speed at 10 m above sea level. However, wind observations are mainly available at the major airports on the west side of the Chesapeake Bay, and conversion of wind on land to wind over water is not an easy task. S. Chao (personal communication, 1996) showed that in order to reproduce the event found in the Chesapeake Bay in April 1986 the longitudinal wind used in the Bay has to be increased compared to the wind measured at Norfolk airport. This increase of wind over water compared to that measured over land has also been pointed out by *Wong and Garvine* [1984] and *Goodrich* [1985]. To explain the sea level in the Delaware Bay, *Wong and Garvine* [1984] had to increase the shore-based wind stress fourfold. *Goodrich* [1985] found that while the longitudinal winds attenuate rapidly toward the shores of the Chesapeake Bay, the lateral winds do not, and that overwater/overland regression slopes for north and east components of the wind are 2.5 and 1.43, respectively.

Tuning wind stress and bottom stress in order to fit the tide gauge observation could quickly become a very tedious task. First, the fitting of the modeled onto the observed M_2 tide does not guarantee an adequate fitting on the K_1 and other components of the tidal signal. Second, fitting at all the tide gauge stations requires numerous model runs. A systematic and objective fitting of model results to observations and determination of wind stress, bottom stress, and exchange between the Chesapeake Bay and the open ocean is accomplished with the use of data assimilation techniques such as variational adjoint or inverse method. Using the variational method, *Yu and O'Brien* [1991] estimated a reasonable wind stress drag coefficient and a vertical eddy viscosity distribution by assimilating wind speeds and current observations. *Das and Lardner* [1992] and *Lardner et al.* [1993] have shown that it is possible to determine the drag coefficient and a correction to the bathymetry using a two-dimensional model and tide gauge observations. *Bang* [1994], using an inverse method and current measurements in the Chesapeake Bay, found a seasonal variation of the drag coefficient between 2.0×10^{-4} and 1.6×10^{-3}.

The goal of this study is to use the variational adjoint method to determine a temporally and spatially varying bottom drag coefficient, wind stress, and open boundary condition at the Chesapeake Bay mouth. Two experiments are considered which achieve this goal. In the first experiment, referred to as the tidal circulation experiment, tidal forcing at the Bay mouth is specified, and the tidal elevation from the major harmonic constituents computed at 10 permanent tide gauge stations is assimilated to estimate the bottom drag coefficient. Using data assimilation for a complete spring-neap tide cycle, it was found that the bottom drag coefficient is larger during neap than during spring tide. The second experiment, referred to as the wind-driven circulation experiment, considers a combined wind and tide problem in which the bottom drag coefficient, wind stress and boundary condition at the Bay mouth are estimated using the actual observations at the ten permanent tide gauge stations. The variation of the bottom drag coefficient during the phase of the tide is largely reduced when the wind reaches speeds > 5 m s^{-1}. While the *Lardner et al.* [1993] study is probably most closely related to our study, several differences are evident. *Lardner et al.* [1993] do not allow a temporal variation of the drag coefficient, the surface forcing was not estimated, and the observations were taken from tide gauges at least 30 km offshore. Taking the data from gauges closer to the shore is indeed far more challenging since the extreme proximity of the coast can yield noisier observations and the model coastline approximations can introduce errors in the modeled elevation.

The description of the assimilation technique, the data, the circulation model, and the definition of the cost function are given in section 2. Section 3 presents the results of the tidal and wind-driven circulation experiment. A discussion of the results is presented in section 4. A summary of the study and conclusions are found in section 5.

2. Methodology

During the past decade, the variational adjoint method has been used largely in meteorology and oceanography to estimate initial and boundary conditions [*Lewis and Derber*, 1985; *Talagrand and Courtier*, 1987; *Thacker and Long*, 1988; *Navon et al.*, 1992]. It has since been used to estimate parameters in circulation models [*Panchang and O'Brien*, 1989; *Das and Lardner*, 1991; *Smedstad and O'Brien*, 1991; *Yu and O'Brien*, 1991; *Zou et al.*, 1992a, b; *Lardner et al.*, 1993; *Spitz*, 1995] and ecosystem models [*Lawson et al.*, 1995, 1996; *Spitz et al.*, 1998]. Two advantages of this technique are that it can be applied to both linear and nonlinear models and that it can be implemented in a straightforward manner. Since the technique has been largely discussed in the literature, we will limit ourselves to a brief overview.

The variational adjoint method determines an optimal solution by minimizing an objective function, the cost function, which measures the misfit between model equivalent to the data and the available observations. Most minimization algorithms are based on iterative descent, large-scale unconstrained, local minimization methods which require the computation of the gradient of the cost function with respect to the control variables, e.g., model parameters being estimated. The computation of the gradient is achieved by using the adjoint model equations which are forced by the model-observation misfits and run backward in time. The data assimilative model, shown in Figure 1, then consists of three components: the forward circulation model, the backward model or adjoint model, and a minimization

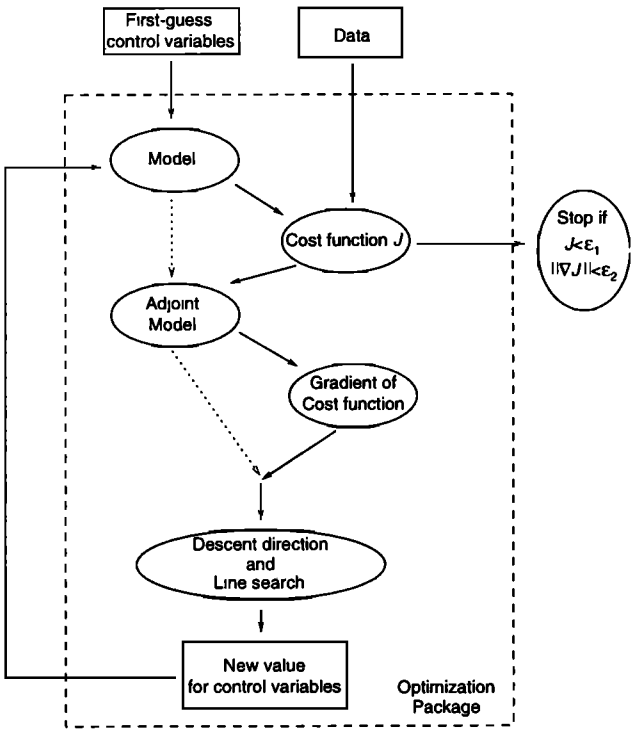

Figure 1. Schematic of the steps involved in the data assimilation scheme. The solid lines indicate the main path taken during the procedure.

procedure. The three components of the assimilative model are used in an iterative procedure which leads to the determination of the control variables giving the best fit to the data and can be described as follows. The direct model is run with an initial guess of the control variables. The model output and data are then used to compute the value of the cost function. Thereafter the adjoint of the model, run backward in time, gives the gradient of the cost function with respect to the control variables (e.g., model parameters), which is then used in the optimization procedure to compute the search direction towards the minimum and the optimal step size in that direction. New values of the control variables are then estimated, and the model is rerun. This procedure is applied until a preset convergence criterion is satisfied, e.g., $J \leq \epsilon_1$ and/or $\|\nabla J\| \leq \epsilon_2$, where ϵ denotes a small value, J is the cost function, and $\|\nabla J\|$ is the norm of the gradient of the cost function with respect to the control variables.

While the adjoint method is a powerful tool for obtaining the gradient of the cost function with respect to the control variables, the most difficult aspect of this technique is the development of the adjoint model code. Two approaches can be taken. The first one consists of deriving the continuous adjoint equations followed by their discretization [*Thacker and Long*, 1988; *Smedstad and O'Brien*, 1991; *Yu and O'Brien*, 1991]. The second one is to derive the adjoint model code directly from the forward model code either using the tangent linear method [*Talagrand*, 1991; *Navon et al.*, 1992] or a technique based upon the use of Lagrange multipliers [*Lawson et al.*, 1995, 1996; *Spitz et al.*, 1998]. The second approach has two main advantages: it provides a straightforward way of writing code and it avoids the inconsistency that can occur from the discretization of the adjoint continuous equations. The tangent linear method was adopted in this study, and a full description can be found in work by *Spitz* [1995].

Any error introduced in the coding of the adjoint model can be devastating. It is then judicious to verify the correctness of the adjoint code and the computation of the gradient of the cost function before any assimilation experiment. Using the tangent linear method, this can be done using the following two verification methods. At any level of the coding of the adjoint model, the correctness can be checked on the basis of the equality of scalar products, $< v, Au >=< A^T v, u >$, where u and v are the input and output vectors, respectively, A is the tangent linear operator, and T denotes the transpose. In other words, the sum of the square of the outputs of either a DO loop or a direct subroutine of the tangent linear code must be equal to the sum of the inputs of that DO loop (direct subroutine) multiplied by the corresponding outputs of the adjoint DO loop (adjoint subroutine), within the limits of computer accuracy. A second verification of the correctness of the gradient of the cost function can be done as follows [*Navon et al.*, 1992]. Perturb the control variable vector by an amount $\alpha\mathbf{U}$ where α is a small scalar and $\mathbf{U}$ is a normalized vector, e.g., $\mathbf{U} = \nabla J/\|\nabla J\|$. The Taylor expansion of the cost function is

$$J(\mathbf{X}+\alpha\mathbf{U}) = J(\mathbf{X}) + \alpha\mathbf{U}^T\nabla_{\mathbf{X}}J(\mathbf{X}) + O(\alpha^2). \quad (1)$$

For

$$\phi(\alpha) = \frac{J(\mathbf{X}+\alpha\mathbf{U}) - J(\mathbf{X})}{\alpha\mathbf{U}^T\nabla_{\mathbf{X}}J(\mathbf{X})},$$

in the limit as α goes to 0, we have

$$\lim_{\alpha\to 0}\phi(\alpha) = 1. \quad (2)$$

Finally, the optimization procedure uses the subroutine N1QN3 from *Gilbert and Lemaréchal* [1989], which is based upon a limited memory quasi-Newton method [*Nocedal*, 1980]. This procedure combines the low storage advantage of the conjugate-gradient method and the computational efficiency of the quasi-Newton method.

2.1. Observations in the Chesapeake Bay

For more than a century, tide and tidal currents have been observed in the Chesapeake Bay. The first tide station was installed in Annapolis in 1844 [*Haight et al.*, 1930; *Hicks*, 1964; *Fisher*, 1986]. Prior to 1964, more than 200 tide gauge stations and over 100 near-surface current stations were deployed. However, they were not usually deployed for a long time or at the same

time. From those stations, 10 tide gauge stations in the Chesapeake Bay and its tributaries are now part of the National Tide and Water Level Observation Network, shown in Table 1 and Figure 2, and are permanent installations maintained by the National Oceanic and Atmospheric Administration (NOAA). In addition to those long-term measurements, two extensive tide and current surveys of the Chesapeake Bay were conducted from 1970 to 1974 and from 1981 to 1983 [*Fisher*, 1986] by the National Ocean Survey (NOS) to update tide and tidal current predictions and to provide tidal datum for shoreline boundary determination. The harmonic constants of the major tidal constituents obtained from those time series [*Fisher*, 1986] are used to create the predicted tidal elevations time series used during the tidal circulation experiment.

For a long time, meteorological observations were collected only at the major airports, e.g., Baltimore; Washington, D. C.; Norfolk International Airports; and Patuxent River Naval Air Station. It is only recently that meteorological observations became available over the water. Starting in 1985, two buoys (Figure 2) were deployed in the Chesapeake Bay by the National Data Buoy Center (NDBC) as part of the Coastal-Marine Automated Network (C-MAN) program. The first buoy is located in the upper Bay at Thomas Point, Maryland (38.9°N, 76.4°W), while the second one is located outside the Bay at the Chesapeake Light Tower, Virginia (36.9°N, 75.7°W). Wind speed, direction, and gust, barometric pressure, and air temperature are processed every hour and transmitted to the users. In addition to those buoys, meteorological observations are available at some tide gauge stations, e.g., at the Chesapeake Bay Bridge Tunnel (CBBT).

2.2. Circulation Model

The circulation model used to study the barotropic circulation in the Chesapeake Bay is a conventional two-dimensional vertically integrated shallow water model. It was developed by the Management Unit of the Mathematical Models of the North Sea and Scheldt Estuary (MUMM) to study the tidal propagation in the English Channel [*Ozer and Jamart*, 1988; *Jamart and Ozer*, 1989] and will be referred to as the MU model.

In a right-handed coordinate system, with the z axis pointing upward, the governing equations are

$$\frac{\partial u}{\partial t} + u\frac{\partial u}{\partial x} + v\frac{\partial u}{\partial y} - fv = -g\frac{\partial \eta}{\partial x} + \frac{\tau_w^x}{\rho H} - \frac{\tau_b^x}{\rho H}, \quad (3)$$

$$\frac{\partial v}{\partial t} + u\frac{\partial v}{\partial x} + v\frac{\partial v}{\partial y} + fu = -g\frac{\partial \eta}{\partial y} + \frac{\tau_w^y}{\rho H} - \frac{\tau_b^y}{\rho H}, \quad (4)$$

$$\frac{\partial \eta}{\partial t} + \frac{\partial (Hu)}{\partial x} + \frac{\partial (Hv)}{\partial y} = 0, \quad (5)$$

where t denotes time, f is the Coriolis parameter, g is the acceleration due to gravity, τ_w^x and τ_w^y are the components of the wind stress, and H is the total water depth. The unknown η is the elevation of the free surface with respect to the mean sea level, and u and v are the east and north components of the vertically averaged velocity, respectively. The bottom stress $\vec{\tau}_b$ is parameterized by means of a quadratic dependence with respect to the depth mean current,

$$\vec{\tau}_b = \rho c_D \|\vec{u}\| \vec{u}. \quad (6)$$

Table 1. Tide Gauge Stations

Station Number	Station Name	Latitude, N	Longitude, W	Installation Date
8574070	Havre de Grace, Maryland	39°46.9′	76°05.5′	1971
8574680	Baltimore, Maryland	39°16.0′	76°34.7′	1902
8575512	Annapolis, Maryland	38°59.0′	76°28.8′	1929
8571890	Cambridge, Maryland	38°34.5′	76°04.3′	1942
8577330	Solomons Island, Maryland	38°19.0′	76°27.2′	1938
8635750	Lewisetta, Maryland	37°59.8′	76°27.8′	1970
8637624	Gloucester Point, Virginia	37°14.8′	76°30.0′	1950
8632200	Kiptopeake, Virginia	37°10.0′	75°59.3′	1951
8638610	Hampton Roads, Virginia	36°56.8′	76°19.8′	1927
8638863	CBBT, Virginia	36°58.1′	76°06.8′	1975

The given National Ocean Service long-term control tide stations are part of the National Tide and Water Level Observation Network. CBBT is the Chesapeake Bay Bridge Tunnel.

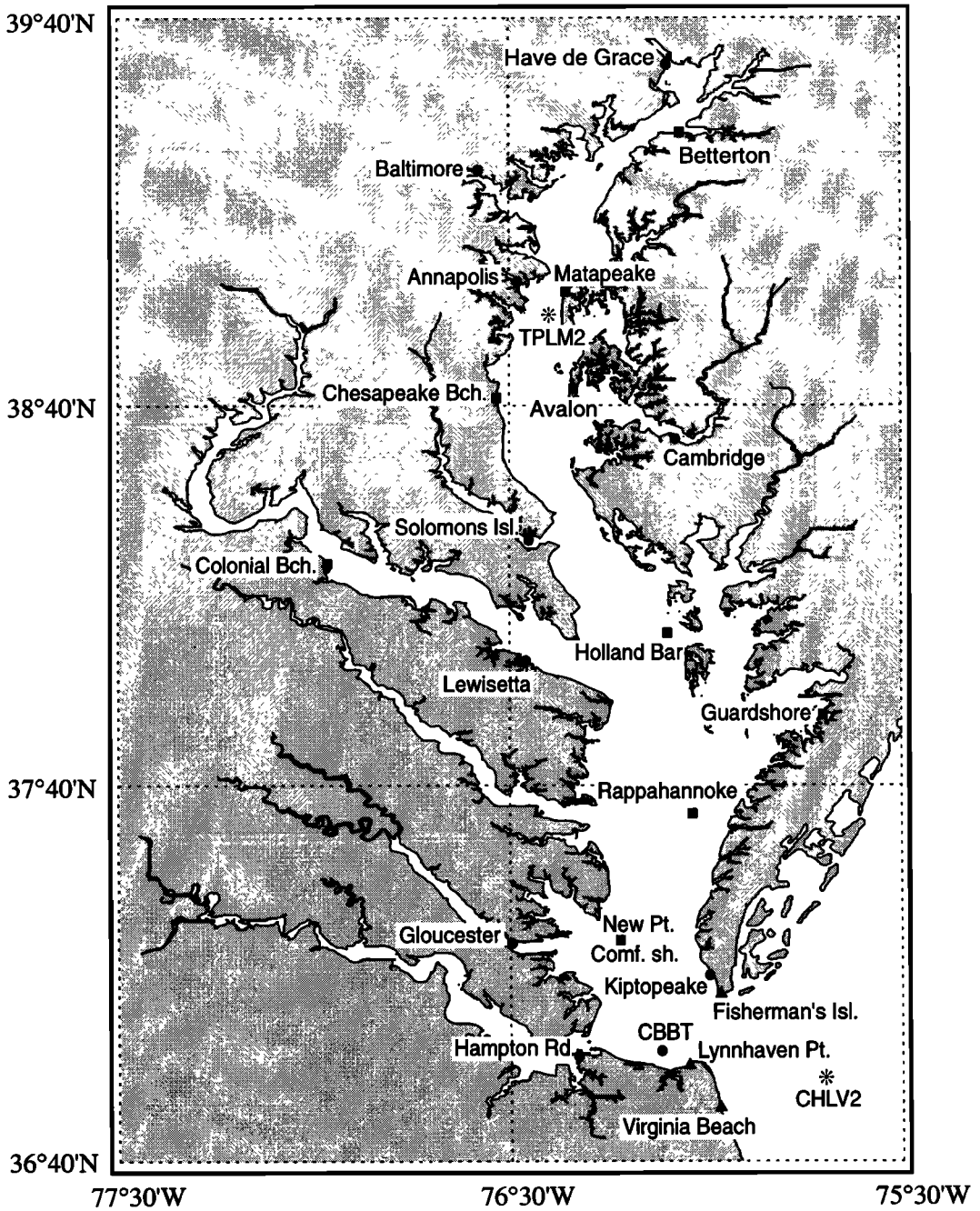

Figure 2. Overview of the tidal stations from the National Tide and Water Level Observation Network (circles), some of the tide gauges from the 1970-1974 and 1981-1983 surveys (squares), and the tide gauges used to compute the elevation at the Chesapeake Bay mouth (triangles). The stars represent the buoys.

In practice, the bottom drag coefficient c_D varies with water depth, seabed composition and phase of the tide. It is parameterized as

$$c_D = \frac{g}{C^2}, \qquad C = \frac{h^\alpha}{n}, \tag{7}$$

where h is the undisturbed water depth, C ($m^{1/2}\ s^{-1}$) is the Chezy coefficient, and n is the Manning's roughness [*Officer*, 1976]. Typical values for α and n are 1/6 and 0.02, respectively, giving a drag coefficient of ~ 0.002 for a depth of 10 m. The two parameters α and n only depend on time and are estimated during the assimilation procedure.

The equations are solved by means of finite difference analogs [*Ozer et al.*, 1990] on a uniform staggered grid (Arakawa C-grid) The time-stepping scheme is a semi-implicit, alternate direction method (ADI) [*Beckers and Neves*, 1985], which is unconditionally stable

and allows larger time steps than permissible by explicit time-differencing schemes such as leapfrog.

Along the open boundaries which coincide with a grid line containing elevation points, the free surface elevation is either determined during the assimilation process for the wind-driven circulation experiment or imposed as follows for the tidal circulation experiment. The forcing due to the tide is introduced by specifying the time evolution of the free surface,

$$\eta(\vec{s},t) = \sum_{k=1}^{K} f_k a_k cos[\omega_k t + (V_o + u)_k - \phi_k], \quad (8)$$

where $\vec{s}$ denotes the position of a point along the boundary, a_k and ϕ_k are the harmonic constants (amplitude and phase) of the kth constituent, ω_k is the frequency of the kth constituent, f_k is a factor to reduce the mean amplitude of the constituent to the starting time of the simulation, $(V_o + u)_k$ is the value of the equilibrium argument of the kth constituent at the starting time of the simulation, and t denotes the time elapsed from the beginning of the simulation. Because of the presence of the advection terms in the momentum equation, an additional boundary condition is necessary at those times when the water flows towards the interior of the domain. In that case, the gradient of the depth mean current in the direction perpendicular to the boundary is set equal to zero along the boundary grid line and along the grid line that is half a grid interval inside the domain.

Along the solid boundaries which coincide with a grid line containing velocity unknowns, the component of the total transport in the direction perpendicular ($\vec{n}$) to the boundary is set equal to zero. The additional condition ($\partial\vec{u}/\partial n = 0$) is applied along the grid line that is half a grid interval inside when the water flows away from the solid boundary.

2.3. Cost Function

The first task in variational data assimilation is to define a cost function suitable for the study under consideration. In a general sense, the cost function takes the form

$$J(\mathbf{X}) = J_o(\mathbf{X}) + J_p(\mathbf{X}), \quad (9)$$

where $\mathbf{X}$ is the control variable vector. J_o measures the distance of the model solution from the observations, and J_p, referred to as penalty term, includes all the physical constraints to be imposed on the model solution.

The first term of (9) is often expressed as

$$J_o(\mathbf{X}) = \frac{1}{2}(C\mathbf{Y} - \mathbf{d})^T \mathbf{W}^{-1}(C\mathbf{Y} - \mathbf{d}), \quad (10)$$

where $\mathbf{d}$ and $\mathbf{Y}$ are the vectors containing the observations and the model variables, respectively, and C is an interpolation matrix which maps the model variables to the space and time locations of the observations. The matrix $\mathbf{W}^{-1}$ is ideally the inverse of the error covariance matrix for the observations. By assuming that errors in the data are uncorrelated and have equal variance, $\mathbf{W}^{-1}$ is then approximated by a diagonal matrix. In that case, J becomes a weighted sum of squares, and the technique simply corresponds to a least squares fit method. In practice, the value of the elements of $\mathbf{W}^{-1}$ are determined by the relative magnitude of the various model variables, their dimensional scaling, and the quality of the data sets.

The addition of a penalty term J_p to the cost function can provide smoother model solutions and estimated parameters and can result in a much faster convergence of the minimization process. *Sasaki* [1970] showed that the penalty term suppresses the high frequencies and wave numbers in the solution. *Courtier and Talagrand* [1990] and *Zou et al.* [1992a, 1993] showed that the penalty term can control spurious gravity waves. *Richardson and Panchang* [1992] and *Lardner et al.* [1993] introduced a penalty term in the cost function in order to penalize large variations in the recovered parameters and to avoid negative drag coefficients. The penalty term might also introduce prior information on the parameters to be recovered and lead to a unique solution [*Carrera and Neuman*, 1986a, b, c].

For the two experiments considered in the present study, the cost function (10), which measures the difference between the model results and the observations, is chosen to be

$$J_o = \frac{1}{2}\sum_{t,s}[\eta(t,\vec{s}) - \hat{\eta}(t,\vec{s})]^2, \quad (11)$$

where t and $\vec{s}$ are the time and location of data and $\hat{\eta}$ and η are the observed sea surface elevation and model-derived values interpolated to the location of the observations. The interpolation scheme is a simple bilinear interpolation. The weight matrix is taken to be the identity matrix so that elevation observations are considered to have equal importance at all the tide gauges in the Chesapeake Bay.

For the wind-driven circulation experiment only (see section 3.2), a penalty term on the wind stress and the open boundary surface elevation was found necessary to ensure the smoothness of the wind field and the surface elevation across the Chesapeake Bay mouth and to accelerate the convergence. Note that the addition of the penalty term does not affect the recovery of the bottom drag coefficient parameters [*Spitz*, 1995]. The penalty term J_p is then defined as

$$J_p = \frac{1}{2}\beta_1 \sum_{k}^{N-1}\left[(\tau^x_{w,k+1} - \tau^x_{w,k})^2 + (\tau^y_{w,k+1} - \tau^y_{w,k})^2\right] + \frac{1}{2}\beta_2 \sum_{t}\sum_{j}^{M-1}[\eta_{b,j+1}(t) - \eta_{b,j}(t)]^2, \quad (12)$$

where τ^x_w and τ^y_w are the components of the wind stress and η_b the surface elevation at the Bay mouth. N and M are the total number of estimated values for the

wind stress and the number of grid points along the open boundary, respectively, and t is the time at which the boundary elevation is recovered. Several identical twin experiments showed that the penalty coefficients $\beta_1 = 0.1$ and $\beta_2 = 0.01$ give the best results; the spatial oscillations in the recovered values are greatly reduced while the spatial structure of the surface elevation at the Bay mouth and of the wind field is preserved.

The necessity of the penalty term on the open boundary elevation was evident from twin experiments even when there was a maximum of observations, i.e., hourly elevation at every grid point [*Spitz*, 1995]. This result suggests that hourly surface elevation in the interior of the Chesapeake Bay does not provide enough information about the boundary elevation, which can be explained as follows. First, the exchange between the open ocean and the Chesapeake Bay through the Bay mouth has a strong influence on the surface elevation in a limited area of the lower Bay ($\sim$ 30 km from the Bay mouth) even though the signal generated at the boundary propagates throughout the entire Bay. Therefore the number of data points containing information about the boundary condition is largely reduced compared to the number of data points containing information on the drag coefficient and the wind stress. The second reason for the necessity of a penalty term is related to the difference in high-frequency signal contained in the data set and the modeled elevation. In the identical twin experiment, the data set was generated using the surface elevation computed with a 10-min time step and then subsampled to a hourly resolution. In this run, the open boundary elevation was imposed with a 5-min resolution which is required by the ADI scheme used to solve the model equations (see details in work by *Spitz* [1995]). During the assimilation process, the model was run with a 10-min time step. The boundary elevation was estimated every hour and then linearly interpolated to a 5-min resolution. Therefore the high-frequency signal contained in the surface elevation near/at the boundary is different for the model results and for the data set. The penalty term then introduces bogus data, which leads to an unambiguous fit to the data in the interior of the Bay and to a smooth elevation across the Bay mouth, and it accelerates the recovery of the boundary elevation. Similar results have been pointed out in several studies [e.g., *Seiler*, 1993], and a full analysis can be found in work by *Thacker* [1988].

3. Tidal and Wind-Driven Circulation Experiments

In both experiments, the model domain, shown in Figure 3, includes not only the main stem but also the tributaries. The grid size is 1′ in latitude ($\Delta y = 1.8$ km) and 1.25′ in longitude ($\Delta x = 2.0$ km), giving grid dimensions of 168 × 68 grid points. The depths at the grid points are interpolated from the NOS 15-s grid data set. In order to keep the problem simple, the river outflows are not taken into account in the simulations, and closed boundary conditions are chosen at the head of the rivers. Therefore the simulations correspond to periods when the river discharges are minimal and can be neglected. At the Chesapeake Bay mouth, the open boundary conditions are either imposed by the tidal forcing defined in (8) (tidal circulation experiment) or assimilated (wind-driven circulation experiment). On the basis of several runs of the direct model, a time step of $\Delta t = 10$ min seems to be appropriate to represent the circulation in the Bay. The adjoint model was run with the same grid spacing, bathymetry, and time step as the forward model. The performance of the data assimilation at a specific location was accessed by computing the following three quantities: the root-mean-square (rms) error defined as

$$\text{rms} = \left\{ \frac{1}{\mathrm{L}} \sum_{\mathrm{i}=1}^{\mathrm{L}} (\eta_{\mathrm{i}} - \hat{\eta}_{\mathrm{i}})^2 \right\}^{1/2}, \tag{13}$$

the relative average error (E) defined as

$$E = 100\% \frac{\sum_{i=1}^{L} (\eta_i - \hat{\eta}_i)^2}{\sum_{i=1}^{L} \left[|\eta_i - \bar{\hat{\eta}}|^2 + |\hat{\eta}_i - \bar{\hat{\eta}}|^2 \right]}, \tag{14}$$

and the correlation coefficient given by

$$r = \frac{\sum_{i=1}^{L} (\eta_i - \bar{\eta})(\hat{\eta}_i - \bar{\hat{\eta}})}{\left(\sum_{i=1}^{L} (\eta_i - \bar{\eta})^2 \sum_{i=1}^{L} (\hat{\eta}_i - \bar{\hat{\eta}})^2 \right)^{1/2}}, \tag{15}$$

where η_i and $\hat{\eta}_i$ represent the time series of the modeled and observed elevation at the considered location, respectively, and an overbar denotes time mean values. L is equal to the number of observations for the considered assimilation window. The root-mean-square and relative average error give a measure of the difference in amplitude between modeled and observed elevations while the correlation coefficient gives a measure of the phase shift. It is important to consider all three of these quantities when evaluating the success of the data assimilation. Indeed, a small relative error with a small correlation indicates a phase shift between the observations and the recovery, an indication of poor performance of the data assimilation procedure.

In all the experiments, hourly surface elevations are assimilated for a period of 24 hours. The choice of the assimilation window was dictated by the timescale of the tidal and wind-driven circulation in the Chesapeake Bay, the limit of the computer capacity, and the validity of the tangent linear model approximation [*Li et al.*, 1993]. An assimilation run with a 24-hour window and recovery of all the forcings of the circulation model typically required over 180 MB of memory and $\sim$ 10 hours of CPU time on an IBM RS-6000/590. An increase of the assimilation window does not significantly

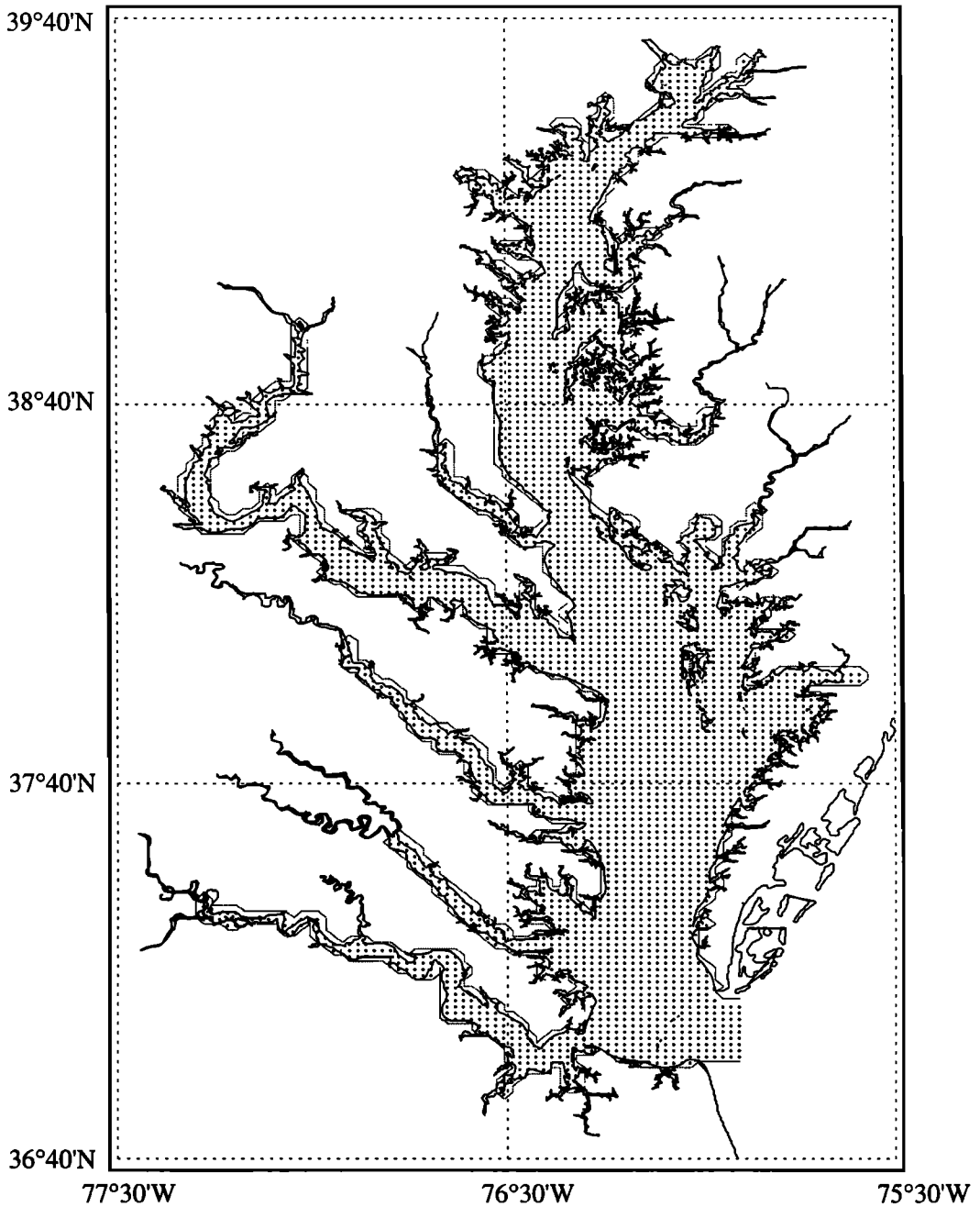

Figure 3. Model domain (dotted line) and grid. The dots inside of the model domain represent grid points.

improve the resolution of the physical processes under study but would have required a larger memory capacity and would have increased the computer time for each run. It was verified that the tangent linear model correctly approximated the nonlinear model in the 24-hour assimilation window.

3.1. Tidal Circulation

The success of recovery of control parameters in the identical twin experiments [*Spitz*, 1995], when the observations are generated by the circulation model, leads us to assimilate real observations from the Chesapeake Bay, and as a first experiment, tidal circulation is investigated. The assimilated data set consists of an hourly time series of sea surface elevation for a period extending from November 1 to 19, 1983, when the most comprehensive set of simultaneous observations is available [*Fisher*, 1986]. The hourly elevation data, referred to as predicted sea surface elevation, are predicted on the basis of five major tidal constituents, M_2, S_2, N_2, K_1, and O_1, using the harmonic constants determined by *Fisher* [1986] at the 10 permanent tide stations (Figure 2).

Nine supplementary tide gauge stations, referred to as comparison stations, are used to compare the modeled surface elevation with the predicted observations.

The two forcings for this experiment are the bottom stress and the tidal forcing at the Bay mouth. The proximity of five tide gauge stations from the Chesapeake Bay mouth allows us to specify the tidal forcing at the open boundary. The surface elevation is computed using (8) and the same five major harmonic constituents used to generate the assimilated data set. The harmonic constants at the Bay mouth are computed based upon the harmonic constants [*Fisher*, 1986] from the five tide gauge stations closest to the Bay entrance (Figure 2): two on the northern end (Kiptopeake and Fisherman's Island; and three on the southern side (CBBT, Lynnhaven Pier, and Virginia Beach). As a result, the M_2 amplitude is chosen to vary linearly across the entrance such that it is 3 cm larger on the northern side than on the southern side of the Bay mouth. The other four harmonic constituent amplitudes are uniform across the Bay mouth. For all the constituents, the phase is taken such that it increases linearly of 5^o from the southern to the northern end of the entrance. Using this definition of the open boundary elevation and adding a 10% perturbation, we found from a twin experiment [*Spitz*, 1995] that the recovery of the bottom drag coefficient parameters was not affected. Consequently, we are confident in using the tidal forcing just described, and the only remaining unknowns in the tidal circulation experiment are the bottom drag coefficient parameters (7).

By definition, the bottom drag coefficient is a function of space through its dependence in h, the undisturbed water depth. While the depth dependent drag coefficient with a typical value for the parameters, $\alpha = 1/6$ and $n = 0.02$, leads to smaller errors than with a uniform drag coefficient of 0.002 (Figure 8 and Figure 9), the temporal variation of the error still remains, especially for the upper Chesapeake Bay stations (e.g., Baltimore and Betterton). Attempts were made to estimate constant parameters but they failed. Temporally varying drag coefficient parameters are then to be estimated during the assimilation process. The time variation of the drag coefficient was introduced by evaluating the parameters $1/n$ and α for a period of 1 day for 18 consecutive days which includes one spring and one neap tide. The actual recovery started on November 2 through 19, 1983, while the recovery for November 1, 1983, was only used to initialize the procedure. Once the bottom drag coefficient parameters were estimated, the direct model was run for 24 hours with the new parameters in order to initialize the circulation for the following day and to compare modeled and predicted elevations. For each day of the recovery experiment, the initial guesses for the parameters $1/n$ and α were taken as their estimated values from the previous day. The assimilation process was stopped when the normalized norm of the gradient of the cost function reached the value of 10^{-6}. This convergence criterion has been determined from the results of November 1 and corresponded to the minimum value that the normalized norm of the gradient of the cost function could attain. For the period under study, convergence occurred after 9-18 iterations, and the cost function decreased an order of magnitude. This small decrease in the cost function is due to the fact that the initial cost function was already small since the recovery was started with the best initial guess.

Predicted and modeled tidal elevations for six typical permanent and six typical comparison tide gauge stations are shown in Figure 4 and Figure 5, respectively. Modeled elevations with the estimated drag coefficients show an excellent agreement with the predicted elevations not only at the permanent stations but also at the comparison stations. In general, the estimated low-tide amplitudes are slightly smaller than the predicted amplitudes in the lower Chesapeake Bay. On the other hand, the recovered high-tide amplitudes are slightly higher than the predicted amplitudes in the upper Bay.

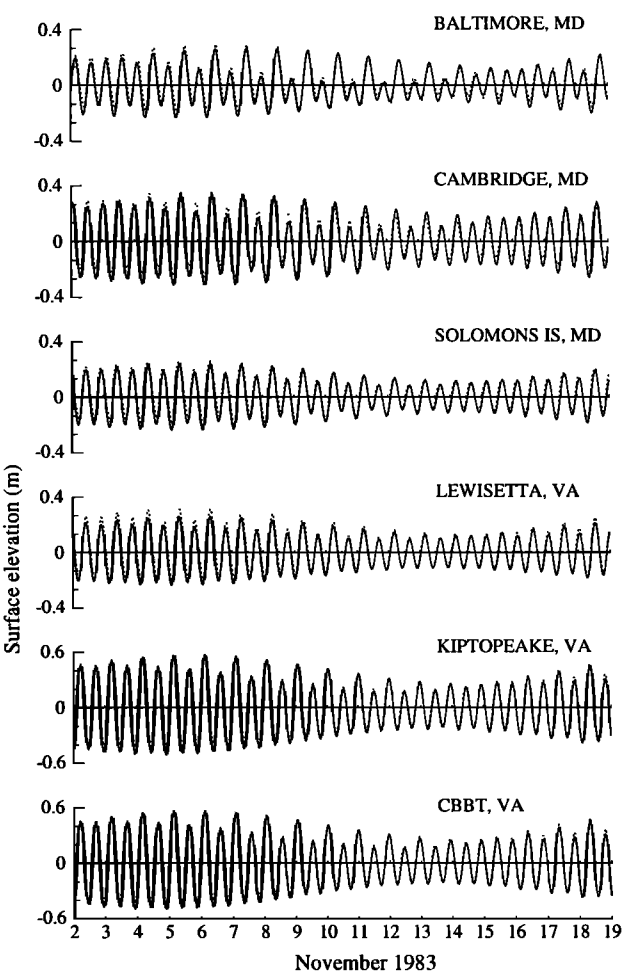

Figure 4. Time series of modeled (dotted line) and predicted (solid line) surface elevation (in meters) at six permanent tide gauge stations. Note the change of scale for the last two stations.

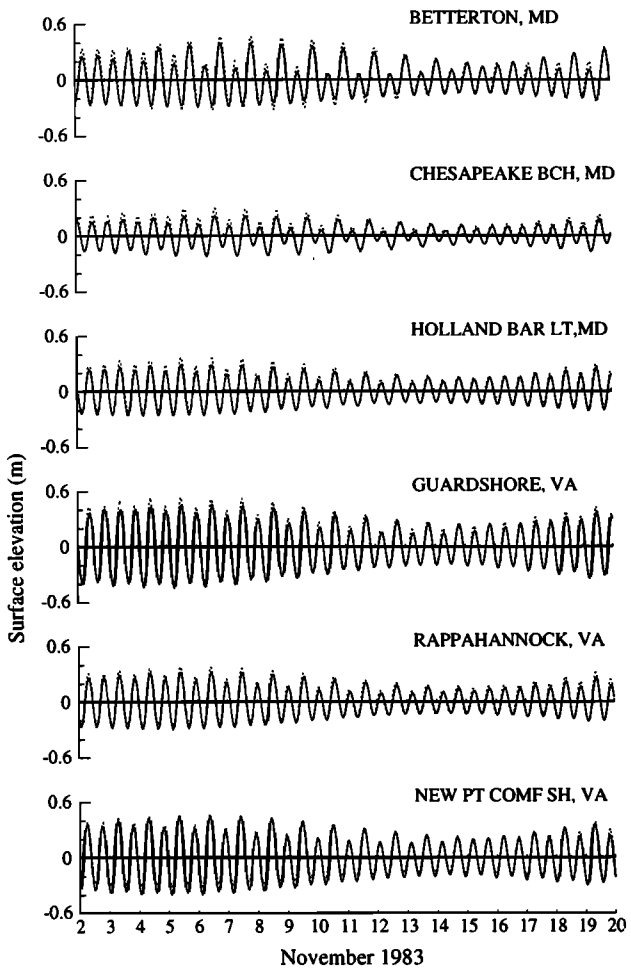

Figure 5. Time series of modeled (dotted line) and predicted (solid line) surface elevation (in meters) at six comparison tide gauge stations.

This difference between modeled and predicted elevations could be due to the fact that the modeled results are linearly interpolated to the tide gauge location. However, differences between modeled and predicted elevations are of the same order of magnitude as the ±2-cm error bounds for datums and mean ranges for the entire Bay [*Swanson*, 1974]. A summary of the root-mean-square error, relative average error, and correlation coefficient for the period of assimilation can be found in Figure 6 and Figure 7. A maximum of $< 7\%$ for the relative average error is found in the main stem while the relative error in the Potomac River (Colonial Beach) reaches a maximum of 9.86%. Using a time and spatially variable bottom drag coefficient largely reduces the error over experiments with only a spatially varying coefficient, shown in Figure 8 and Figure 9. A correlation coefficient > 0.96 is found in the main stem, and a minimum correlation coefficient equal to 0.91 is found in the Potomac River. This indicates a very small shift between modeled and predicted elevations, which could result from the fact that modeled elevations have been linearly interpolated in space to the location of the tide gauge. Finally, it should also be pointed out that the same agreement is found at Havre de Grace despite the fact that the station is near the Susquehanna River, which has the biggest discharge of all rivers.

Using harmonic analysis for the time series of the modeled elevations with the estimated drag coefficients between November 2 and 19, the amplitude and phase of the M_2 and K_1 tide at every grid point of the model domain were computed. A comparison between the M_2 coamplitude chart from *Fisher* [1986] and the corresponding chart for the modeled M_2, seen in Figure 10, shows a very good agreement. The same agreement (not shown) was found for the K_1 tide. The M_2 coamplitude lines run across the Chesapeake Bay at the entrance, then become longitudinal, and finally run across the Bay in the upper Bay. The M_2 amplitude decreases from the Bay mouth towards the main stem and then increases north of Baltimore. The amplitude of modeled M_2 tide is slightly larger than the amplitude found by *Fisher* [1986], which can be attributed to the fact that the time series of modeled elevations (18 days) was too short to fully separate the M_2, N_2, and S_2 tides. A comparison between the M_2 cophase chart from *Fisher* [1986] and modeled M_2 cophase chart, seen in Figure 11, again shows excellent agreement. For example, the 310° cophase line goes through Rappahannock in both cases. The cophase lines are uniformly spaced in the lower Bay. In the upper Bay, the cophase line spacing decreases in the narrow portions and increases in the wider portions. The fact that the curvature of the recovered cophase lines at the entrance of the Bay is not as pronounced as the curvature found by *Fisher* [1986] is due to the imposed boundary condition at the Bay mouth. The predicted elevation was taken linearly across the Bay mouth, which does not allow any curvature of the cophase lines. Two virtual amphidromic points, i.e., near the Severn River (north of Annapolis, Figure 2) and the Potomac river, are evident. At those locations, the coamplitude lines are concentric, and the cophase lines converge. Those two points were also found by *Browne and Fisher* [1988].

While predicted and modeled elevations are in excellent agreement, probably the most interesting feature resulting from the assimilation process is the periodicity of the estimated inverse Manning's roughness while the exponent α (7) is mainly constant during the entire assimilation period. As a result, the bottom drag coefficient, shown in Figure 12, is smaller during spring tide (days 5-6) than during neap time (days 14-15). That difference is accentuated as the depth decreases. The estimated bottom drag coefficient varies between 2.5×10^{-4} and 3.1×10^{-3}. Using an inverse method and tidal-current observations in the lower and upper Chesapeake Bay, *Bang* [1994] found a similar range of values for the bottom drag coefficient, i.e., $2.0 \times 10^{-4} \leq c_D \leq 1.6 \times 10^{-3}$. This variation in the bottom drag coefficient can be related to a variation in the bottom roughness length following *Mofjeld* [1988]. On

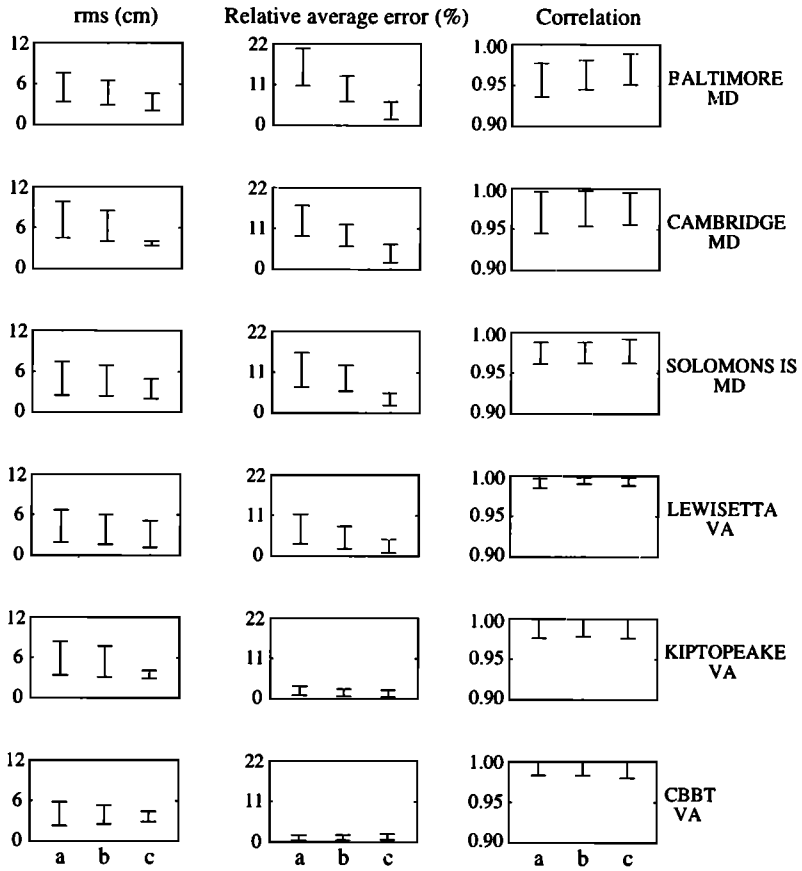

Figure 6. Range of the root-mean-square error (in centimeters), relative average error (%), and correlation coefficient between November 2 and 19, 1983, at six permanent tide gauge stations. Case a corresponds to the results with $c_D = 0.002$, case b corresponds to the results with spatially varying c_D, and case c corresponds to the results with the estimated c_D from the assimilation process.

the basis of the non-rotating channel theory in which frictional drag balances barotropic pressure forcing and shear production of turbulence is balanced by local dissipation (closure of level 2), *Mofjeld* [1988] found that the bottom drag coefficient is given by

$$c_D = \frac{\kappa^2}{\left[\log\left(\frac{H}{z_o}\right) - 1\right]^2}, \tag{16}$$

where $\kappa = 0.4$ is the von Karman constant, z_o is the bottom roughness length, and H is the total water depth. Using (7) and (16) and an average depth of 8 m, the bottom roughness length is found to be equal to 0.01 cm during neap tide and 0.0001 cm during spring tide. This is in the range of the values found by *Wright et al.* [1992]. A Similar range from 0.00005 to 1.5 cm for the bottom roughness was found in the Irish Sea by *Green and McCave* [1995]. In order to get a more accurate estimate of the bottom roughness, the relation (16) should be used in the circulation model and z_o should be estimated during the assimilation process.

3.2. Wind-Driven Circulation

Since modeled tidal circulation in the Chesapeake Bay has shown to be considerably improved by using variational data assimilation, our next focus is on wind-driven circulation, which is harder to model. Wind-driven circulation in the Chesapeake Bay was investigated by assimilating hourly sea surface elevation observations from the 10 permanent tide gauges (Figure 2) between November 2 and 8, 1990. Note that the period of assimilation is different from the tidal circulation experiment. During the year 1983 (tidal circulation experiment), wind observations over the Chesapeake Bay were not available. However, in 1990, hourly wind speed and direction observations were available at two buoys deployed by NOAA (Figure 2), Thomas Point and Chesapeake Light Tower, and at the tide gauge station CBBT, making a comparison between observed and estimated wind possible.

During the chosen assimilation period, either a southwesterly or southeasterly wind, shown in Figure 13, persisted for about 4 days over the entire Chesapeake Bay

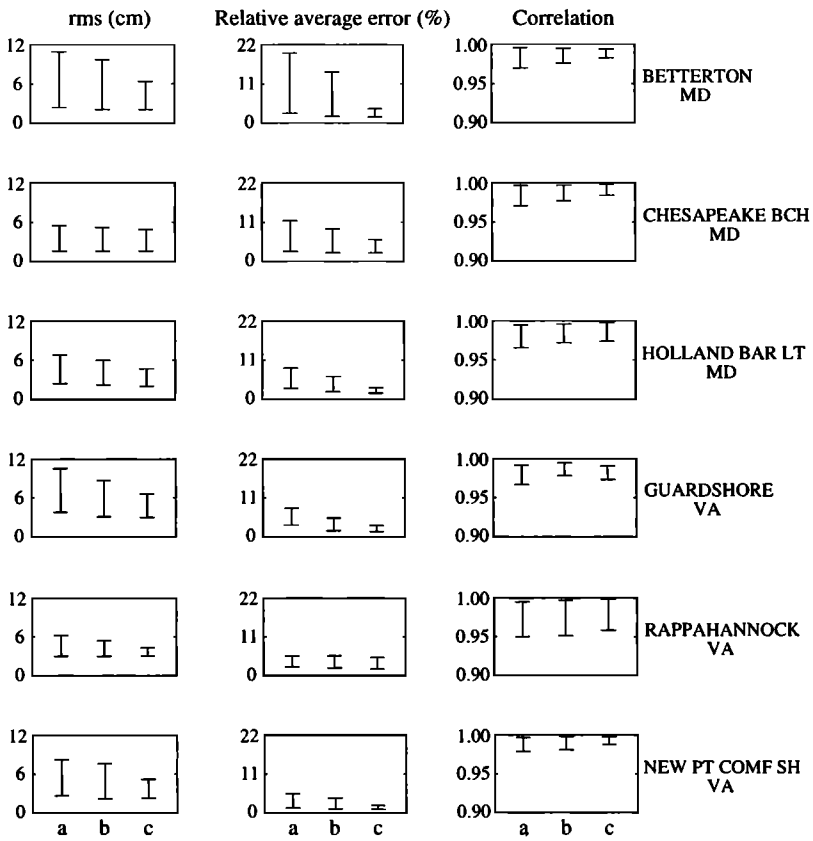

Figure 7. Range of the root-mean square-error (in centimeters), relative average error (%), and correlation coefficient between November 2 and 19, 1983, at six comparison tide gauge stations. Case a corresponds to the results with $c_D = 0.002$, case b corresponds to the results with spatially varying c_D, and case c corresponds to the results with the estimated c_D from the assimilation process.

with a speed < 5 m s^{-1} in the upper Bay and slightly higher in the lower Bay. During those few days, a sea breeze pattern is also noticeable. In the afternoon of November 5, the wind speed increased to about 10 m s^{-1} in the upper Bay. An increase of the surface elevation is immediately noticeable in the upper Bay; for example, the high-tide elevation is about twice its predicted value at Baltimore (Figure 15). A smaller change in the surface elevation can also be seen at CBBT. On November 6, a change of the wind direction associated with the passage of a cold front is evident. The wind became northwesterly in the upper Bay and northeasterly in the lower Bay. Again, a similar effect of the wind direction change can be seen in the observed surface elevation at both stations. The surface elevation decreased in Baltimore and increased at CBBT, which are the expected responses to a northwesterly and a northeasterly wind, respectively. This change in the surface elevation is larger on November 8 when the wind become stronger. Finally, notice that the wind direction outside of the Bay (Chesapeake Light Tower) is roughly the same at CBBT while the wind speed is slightly larger. Therefore we do not anticipate any different behavior in the surface elevation from the Bay mouth and at CBBT.

The time variations of the wind stress and the bottom drag coefficient parameters were introduced in the recovery experiment by evaluating the parameters for a period of 1 day for 7 consecutive days. Since the wind over the Chesapeake Bay changes over a period of 2-3 days, the wind stress components are taken to be constant during the 24-hour assimilation and are estimated for 7 consecutive days. The wind stress components are estimated at four locations in the north-south direction while they are kept uniform in the east-west direction. They are then linearly interpolated in space to get an estimate at every grid point. The first location where wind stress components are evaluated corresponds to the Chesapeake Bay Bridge Tunnel (CBBT) station, and the other three locations are taken 80 km apart in the north-south direction. The sea surface elevation is recovered hourly at every grid point along the open boundary and therefore contains the signal due to the tidal and wind forcing across the Bay mouth. Since these elevation values are required at every half time step (ADI scheme), the hourly values are linearly interpolated in time. As a first approximation, the inverted barometer effect is neglected in this study, even though it can at times become important [*Paraso and Valle-*

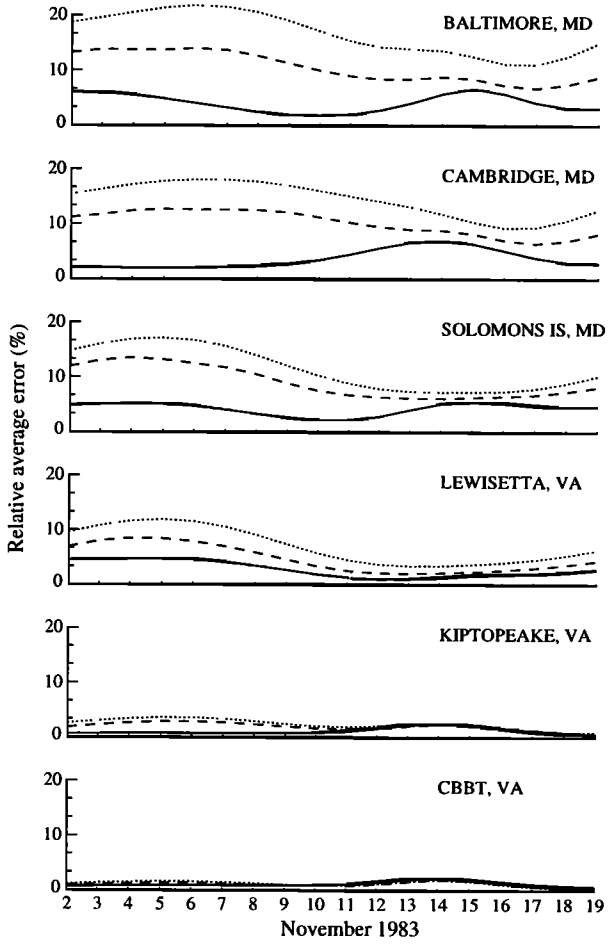

Figure 8. Time series of relative average error (%) at six permanent tide stations. The solid line corresponds to the recovered surface elevations, the dotted line corresponds to the modeled elevations with $c_D = 0.002$, and the dashed line corresponds to the modeled elevations with a typical spatially varying drag coefficient ($\alpha = 1/6$ and $n = 0.02$).

Levinson, 1996]. For the considered period, the largest temporal variation of the air pressure happened during two days with a decrease of $\sim$ 10 mbar on November 5 and an increase of the same order of magnitude on November 6. There was also no attempt to remove any air pressure signal from the tide gauge elevations since this information was not available at most of the stations.

The actual recovery started on November 2 through 8, 1990, while the estimated parameters for November 1, 1990, were only used to initialize the procedure. Once the bottom drag coefficient parameters, wind stress, and boundary conditions were estimated, the direct model was run for 24 hours with the new parameters in order to initialize the circulation for the following day and to compare modeled and predicted elevations. For each day of the assimilation experiment, the initial guess for the control variables was taken as their estimated value from the previous day. The recovery was stopped when the normalized norm of the gradient of the cost function reached a value of 10^{-3}, which is a higher value than for the tidal experiments. The assimilated data are indeed actual observations and are noisier than the data used in the tidal recovery. For each day of assimilation, the cost function decreased 1 order of magnitude. As for the tidal experiment, the small decrease in the cost function can be attributed to the fact that the assimilation runs were started with the best initial guess. The number of iterations necessary to satisfy the preset convergence criterion varied between 244 and 370. The cost function decreased rapidly during the first 30 iterations and continued to slowly decrease until convergence was reached. This pattern was also found for the identical twin experiments [*Spitz*, 1995].

Time series of modeled sea surface elevation is shown in Figure 14. Excellent agreement between estimated and observed surface elevation is evident for the entire period of assimilation in the lower Chesapeake Bay. In

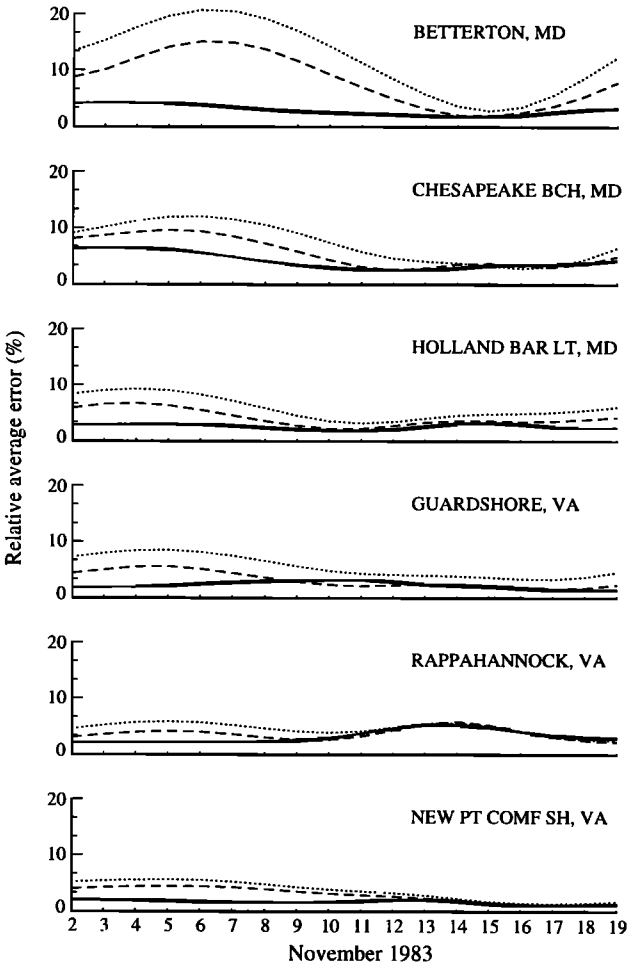

Figure 9. Time series of relative average error (%) at six comparison tide stations. The solid line corresponds to the recovered surface elevations, the dotted line corresponds to the modeled elevations with $c_D = 0.002$, and the dashed line corresponds to the modeled elevations with a typical spatially varying drag coefficient ($\alpha = 1/6$ and $n = 0.02$).

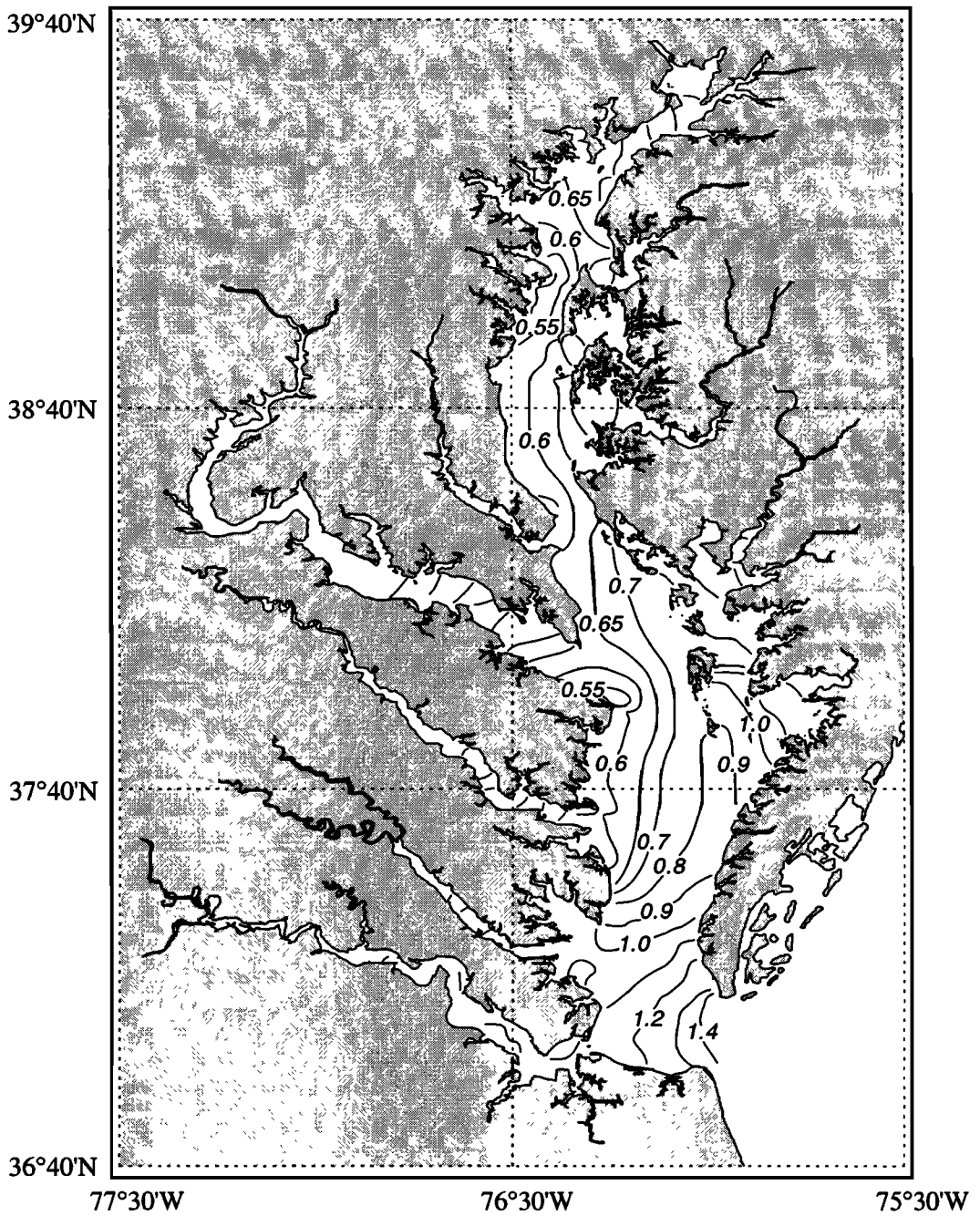

Figure 10. Coamplitude of the recovered M_2 tide expressed in feet.

general, a relative average of error < 3% is found for the stations in the lower Bay, and the correlation coefficient is over 0.99. In the upper Bay, the agreement is also very good until the frontal passage. The relative average error is < 5% until November 6 when it increases to about 15%. While the correlation coefficient is over 0.9, a variation in its value is also noticeable for the same period.

Estimated daily wind vectors at Thomas Point and CBBT for November 2-8, 1990 are plotted in Figure 15 and Figure 16, respectively. Wind speed and direction were obtained from the wind stress components using a quadratic law with a drag coefficient of 2.0×10^{-3} [*Schwab*, 1982]. The wind pattern is well represented in the lower Chesapeake Bay. At CBBT, the estimated wind is mainly southwesterly and shows an increase of magnitude late on November 5. A change of direction occurs on November 6, which is in agreement with the observed wind pattern. In the upper Bay, the agreement is not as good until the frontal passage, when the wind speed increased to 10 m s^{-1} and a change in direction occurred. This suggests that during periods of weak wind, mechanisms other than the local wind forcing are more important in the narrowest part of the Bay.

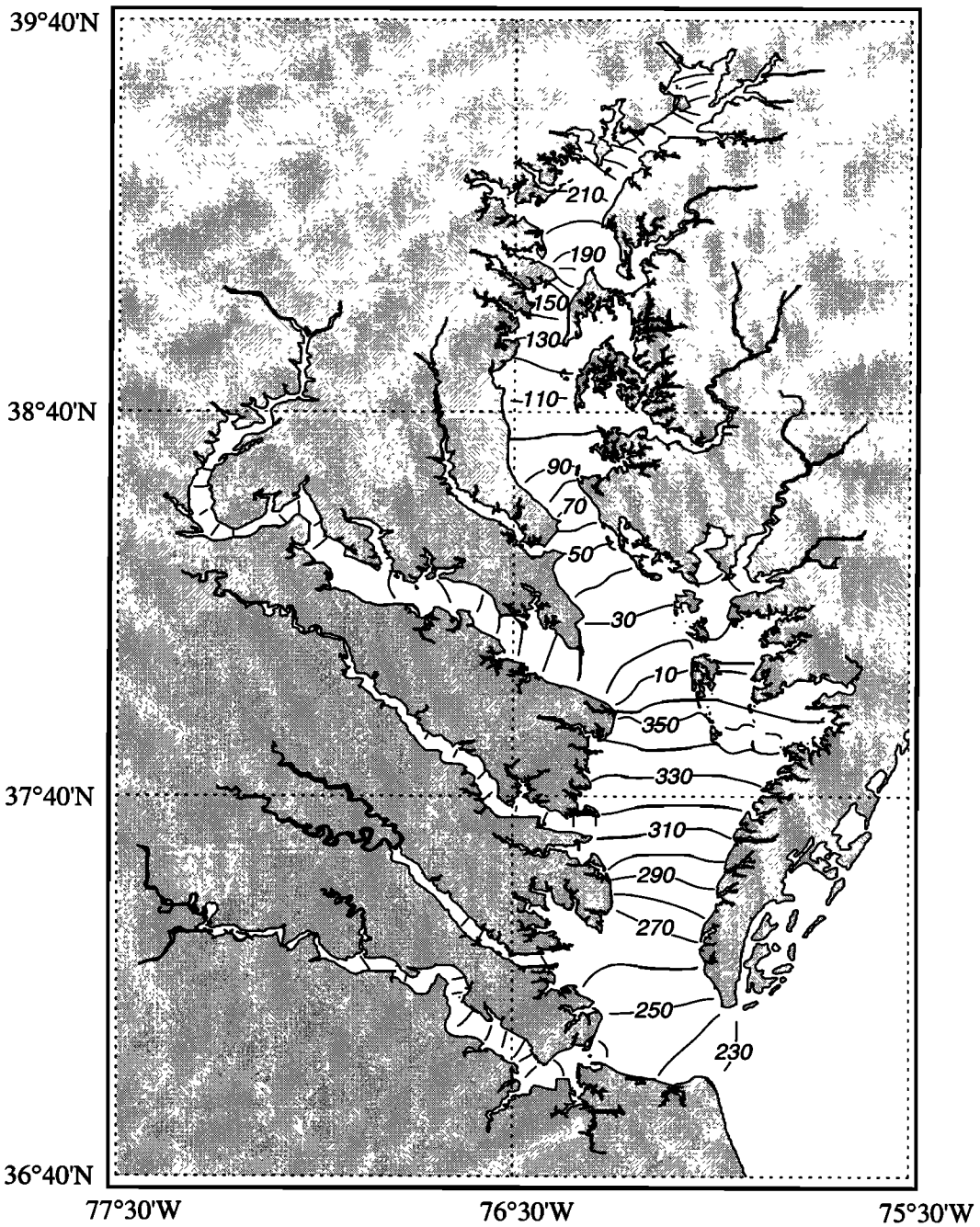

Figure 11. Cophase of the recovered M_2 tide expressed in degrees.

The recovered drag coefficient, seen in Figure 17, shows a minimum on November 5, which corresponds to the period of spring tide. This is followed by an increase until November 6, when there is a frontal passage. The drag coefficient then decreases and reaches roughly the same value regardless of the depth of the considered region in the Chesapeake Bay. While a continuous increase of the drag coefficient was expected until neap tide, northwesterly and northeasterly winds seem to decrease the magnitude of the drag coefficient compared to its value with no wind or southeasterly wind.

The estimated boundary elevation at the Chesapeake Bay mouth displays the expected behavior. The high-tide elevation is higher and the low-tide is lower on the northern end of the Bay mouth than at the southern end. This difference in elevation decreased when the wind changed direction and blew from the northwest and the northeast. The elevation at the northern end of the Bay mouth is slightly higher than the expected value. This can be due to the fact that the boundary region in our model is about half the width of the real boundary, which would take into account the widening of the Bay at its southern end.

As additional evidence of the improvement of the modeled wind-driven circulation by using data assimilation, the recovery experiment (not shown) has been

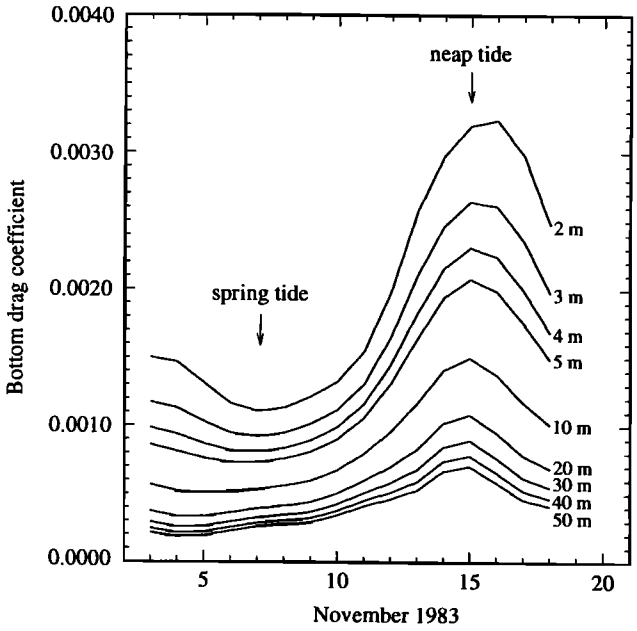

Figure 12. Time series of estimated bottom drag coefficient c_D for depths between 2 and 50 m.

repeated for September 20 and 21, 1983. During that period of time, sea level measurements are also available at tide gauges other than the permanent tide gauges. It was then possible to compare modeled and observed surface elevations from tide gauges other than the one used during the assimilation process. Unfortunately, the wind observations are only available at the major airports, and comparison between estimated and observed wind is very difficult. During the considered period of time, a dominant effect of the wind on the surface elevation can be seen. One should also point out that at the same time, there was a destratification of the Chesapeake Bay [*Blumberg and Goodrich*, 1990]. Therefore the circulation during those 2 days should be well represented by our barotropic model. Modeled and observed surface elevations (not shown) show a very good agreement not only at the permanent but also at comparison tide gauges. Furthermore, the magnitude and direction of the recovered middle Bay wind, i.e., southwesterly wind, was found to be comparable to the wind measured at the Patuxent River Naval Air station [*Blumberg and Goodrich*, 1990]. This experiment indicates that the modeled wind-driven circulation in the main stem can be improved by assimilating only the surface elevations measured at the 10 permanent tide gauges.

4. Discussion

This study represents the first attempt to use surface elevations from tide gauges to estimate the bottom and surface forcings in the Chesapeake Bay. Although the circulation model did not include stratification, river runoff, or the inverted barometer effect and the number tide gauge stations was limited to 10 permanent stations, the modeled surface elevations with the estimated drag coefficient, wind stress, and boundary conditions at the Bay mouth are in excellent agreement with the observations at the 10 permanent tide gauge stations. The temporal variation of the drag coefficient and the effect of the wind on that coefficient have been clearly shown in the results of the tidal and wind-driven experiments. This result can also be supported by the work of *Lardner et al.* [1993]. While the temporal vari-

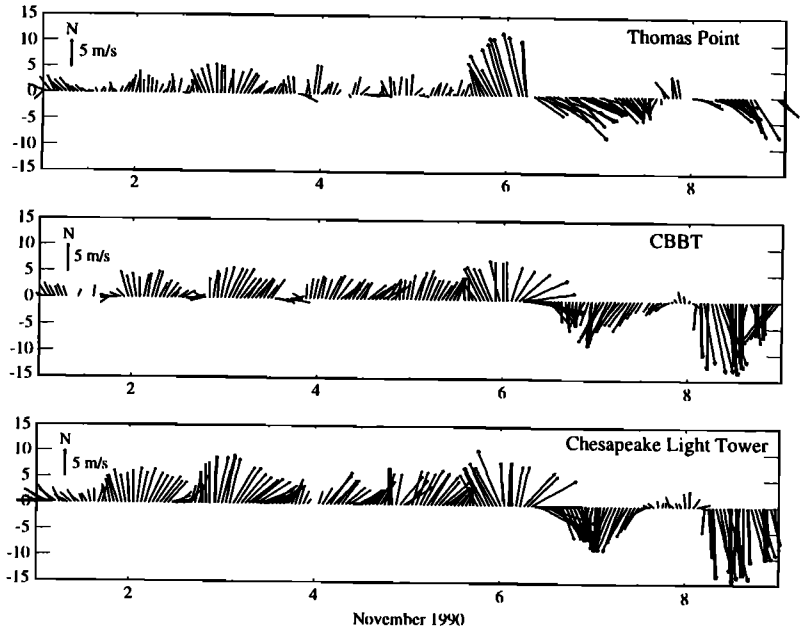

Figure 13. Hourly observed wind in November 1990 at two buoys, Thomas Point and Chesapeake Light Tower, and at the tide gauge station Chesapeake Bay Bridge Tunnel (CBBT). The stick diagram is plotted using the oceanographic convention.

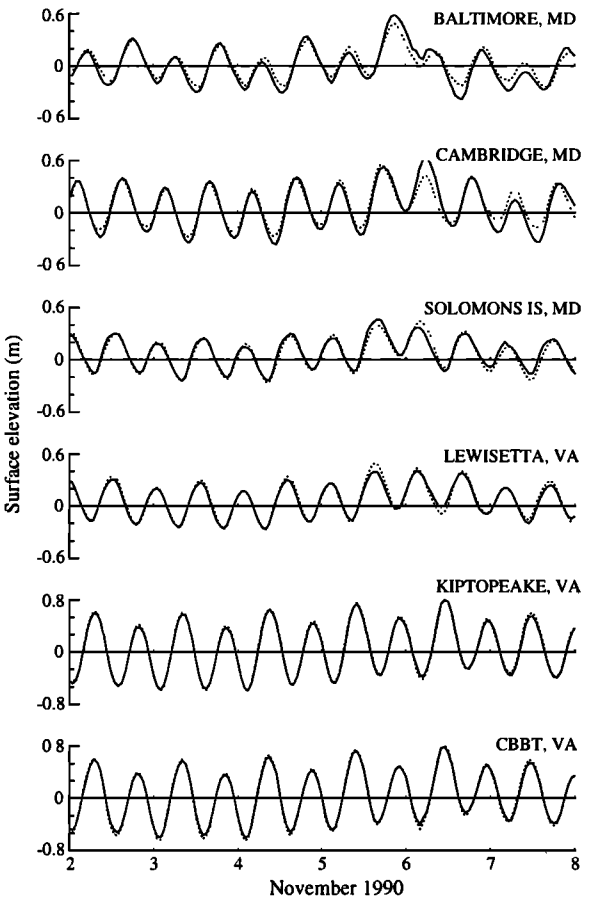

Figure 14. Time series of modeled (dotted line) and observed (solid line) surface elevation (in meters) at six permanent tide gauge stations.

ation of the drag coefficient was not taken into account by *Lardner et al.* [1993], the rms error found at various stations in the Arabian Gulf is higher during spring tide than neap tide, which would lead to the proposition that a temporal variation of the drag coefficient is true not only for the Chesapeake Bay but also for other bodies of water. Finally, the atmospheric forcing has been shown to have different signatures in the upper and lower Bay.

4.1. Temporal Variation of the Bottom Drag Coefficient

In the present study, the bottom drag coefficient was defined in terms of a Chezy coefficient (i.e., it depends on the total depth) and a roughness coefficient (7). A systematic adjustment of the drag coefficient was first done by assimilation of predicted tidal elevations and estimation of the two free parameters, i.e., the exponent of the total depth and the inverse of the roughness, when the tidal forcing was imposed at the Chesapeake Bay mouth. In the tidal experiment, by assimilating the predicted tidal elevation on 24 hours for 19 consecutive days, temporal variation of the drag coefficient for a spring-neap tide cycle was allowed. From the tidal elevation assimilation experiment, it is found that the bottom drag coefficient displays a periodicity corresponding to the fortnightly modulation. The drag coefficient varies between 2.5×10^{-4} and 3.1×10^{-3} with a minimum value at spring tide and a maximum at neap tide. While the lower value seems to be smaller than the value found in the literature related to tidal modeling [*Ronday*, 1976; *Johns*, 1983; *Werner and Lynch*, 1987; *Crean et al.*, 1988; *Ozer and Jamart*, 1988], a similar range was found by *Bang* [1994] in his study in the Chesapeake Bay. Similarly, *Green and McCave* [1995] found a high variation from 0.0008 to 0.01 in the seabed drag coefficient under tidal currents in the Irish Sea. The study of wind-driven circulation shows that the bottom drag coefficient decreased during strong northeasterly and northwesterly wind compared to its value without wind or with a weak wind (Figure 12 and Figure 17).

In the tidal circulation experiment, the tidal forcing at the entrance of the Chesapeake Bay was imposed based upon the harmonic constituents used to generate the data set and for which phase and amplitudes were computed from five tide gauge stations harmonic constants. After verifying that a perturbation in the tidal forcing did not affect the recovery of the drag coefficient parameters (not shown), we were able to refute the hypothesis that the temporal variation of the drag coef-

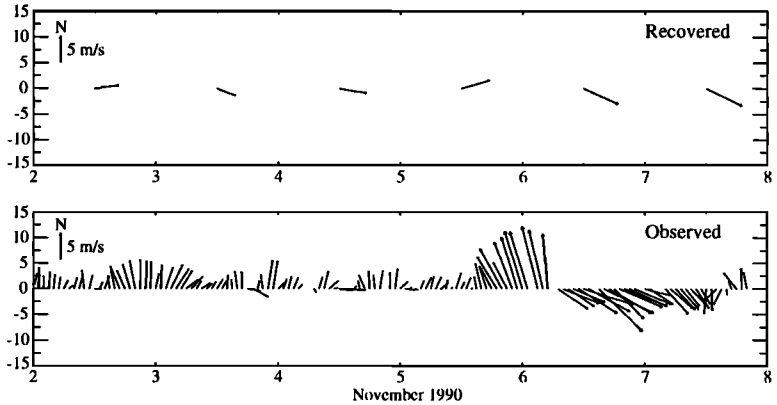

Figure 15. Recovered and observed wind at Thomas Point. The recovered wind, plotted at the middle of the recovery day, is constant during that day.

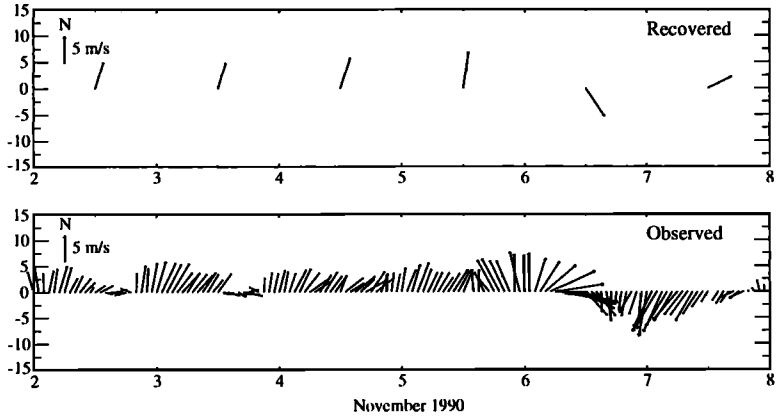

Figure 16. Recovered and observed wind at CBBT. The recovered wind, plotted at the middle of the recovery day, is constant during that day.

ficient parameters could result from a poor definition of the open boundary condition. We are then left with two plausible causes for the fortnightly modulation of the bottom drag coefficient. The first plausible cause for the temporal variation of the drag coefficient can be attributed to the variation of the bottom roughness. This effect can lead to a variation of the drag coefficient during strong wind periods. Indeed, several studies [*McCave*, 1973; *Taylor and Dyer*, 1977; *Grant and Madsen*, 1982; *Davies*, 1983; *Gross and Nowell*, 1983; *Wright et al.*, 1992] showed temporal variability of the bottom drag coefficient due to variation in roughness elements such as ripples and biogenic micromorphology, in movable bed roughness caused by sediment transport, and in interactions between waves and currents. Although the temporal changes of the bottom roughness in the Chesapeake Bay are not yet well understood, *Wright et al.* [1992] found seasonal variability due to biological processes controlling bed micromorphology and variation at a period of a few hours due to wave activity. The variation in the bed roughness with wind has been also shown by *Wright et al.* [1992], who argued that strong winds should be able to generate 5-s waves large enough to agitate the bed at depth of 10-12 m in the Bay and yield variations in the bottom roughness.

A second cause that would account for the periodicity of the bottom drag coefficient can be related to the level of stratification. It has been shown that mixing in the lower Chesapeake Bay and tributaries appears most intense at spring tide while stratification appears most highly developed at neap tide [*Haas*, 1977; *Valle-Levinson*, 1995]. At spring tide, the vertically averaged current and the bottom current are of the same order of magnitude while the vertically averaged current is smaller than the bottom current at neap tide. Since the bottom stress in our model is defined in terms of the vertically averaged current, the drag coefficient must be larger during neap tide than during spring tide in order to compensate for the difference between averaged and bottom current assuming that the bottom drag is the same. The effect of stratification on the bottom drag coefficient has been studied by *Ullman and Wilson* [1998] in the Hudson estuary by assimilating ADCP data collected from a moving vessel during a 5-day period (April 29 to May 3, 1993) and along a 10-km stretch. They found that an increase (decrease) of stratification during neap (spring) tide results in a decrease (increase) in the bottom drag coefficient. The drag coefficient increased $\sim$ 30% from neap to near-spring tides due to a change in stratification of $\sim$ 10-15 sigma over a depth of 25 m. In November 1990, the stratification in the Chesapeake Bay is roughly 1-2 sigma in the ship channels (10 m deep) and almost zero over the flats (A. Valle-Levinson, personal communication, 1996). Therefore the stratification effect on the variations of the bottom drag coefficient is largely reduced in the Chesapeake Bay compared to the Hudson estuary. This suggests that the temporal variations

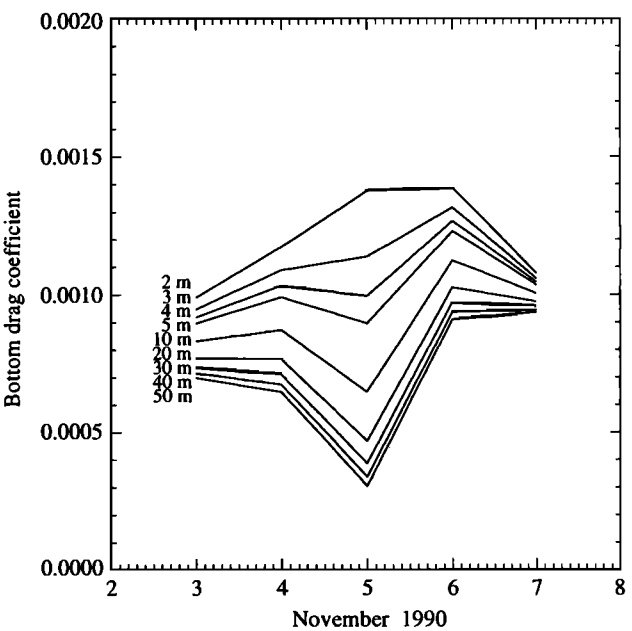

Figure 17. November 1990 time series of recovered bottom drag coefficient c_D for depths between 2 and 50 m.

of the bottom drag coefficient in the Chesapeake Bay would be strongly related to the variations in the bottom roughness and would be lower during spring tide because of an increase of the bottom roughness. This is also in agreement with the conclusions of *Green and McCave* [1995] when they analyzed similar observations in the Irish Sea. The stratification effect could, however, explain the fact that while in the tidal experiment, the temporal trends of the drag coefficient are similar in both the shallow region and deep channel (Figure 12); they are opposite in the wind-driven experiment (Figure 17). Indeed, the stratification effect is not included in the tidal prediction (tidal experiment) but is included in the real observations (wind-driven experiment).

The variation in the drag coefficient during strong wind periods can also be related to the level of stratification. During frontal passage, the water column becomes less stratified, indeed destratified [*Blumberg and Goodrich*, 1990]. Therefore bottom velocity and vertically averaged velocity approach the same value. Finally, similar wind effect on the bottom friction was found by *Ronday* [1976] for his study of the North Sea. He showed that a term proportional to the wind stress had to be subtracted from the bottom stress in order to match modeled and observed elevation when the drag coefficient was taken equal to its value without wind. For a northeasterly wind, this corresponds to an increase of the bottom stress, which can also be achieved by a decrease of the bottom drag coefficient.

4.2. Atmospheric Forces in the Chesapeake Bay

The second important feature noticed during the wind-driven circulation experiment is the relative importance of the driving forces in the Chesapeake Bay. While the modeled surface elevation is in excellent agreement with the observed elevations in the main stem, the estimated wind speed and direction in the upper Bay are not in as good agreement with the observations as in the lower Bay. Thomas Point buoy, which is situated at the narrowest portion of the Bay (Figure 2), was used to compare the modeled results with the observations in the upper Bay, and CBBT tide gauge station was used in the lower Bay. Near Thomas Point, the main stem changes its orientation from northwest-southeast to northeast-southwest and becomes shallower. During periods of weak wind, the topographic and narrowing effect should be dominant. The model grid spacing, roughly 2 km, is probably too large to correctly resolve the influence of the narrowing of the Bay. Instead, the correction is done to the wind stress in order to minimize the data misfit at Annapolis, which is the closest tide gauge station. When the wind becomes stronger, as in the case during a frontal passage, the surface elevation response to the wind is larger and the wind signal in the observations is also stronger. In those conditions, estimated and observed wind speed and direction are in excellent agreement. Further investigation with a finer grid than 2 km is needed to fully investigate the circulation in that area.

A second effect that is neglected and could be a cause for the disagreement between estimated and observed wind is the inverted barometer effect, which induces an increase of the surface elevation for a low-pressure system and a decrease of the surface elevation for a high-pressure system. For example, *Paraso and Valle-Levinson* [1996] showed that for February 10-11, 1992, the barometric pressure rise contributed 57% to the sea level change at CBBT and, in general, the effects of the atmospheric pressure on sea level are not negligible. *Vieria* [1986] found that the 2-2.5-day sea level oscillations in mid-Bay could not be identified with a seiche in the Bay but could be due to the atmospheric pressure. During the period corresponding to our study, changes in the barometric pressure are also important. From November 1 to 3, 1990, the atmospheric pressure was about 1023 mbar. It then decreased to a minimum of 1002 mbar on November 6 after which it increased to a maximum of 1022 mbar in the afternoon of November 7. High pressure during the first 3 days of November acted to decrease the surface elevation near Thomas Point and acts against the effect of the wind. The inverted barometer effect, not included in our model, is accounted for through modification of the wind speed and direction. Also, this effect is likely to contribute to the model/data misfit increase on November 6 at Baltimore and Cambridge (Figure 14).

In order to improve the estimated wind field in the Chesapeake Bay, two remedies can be proposed. First, since it has been shown that the inverted barometer effect is not negligible in general [*Paraso and Valle-Levinson*, 1996], a natural extension of the MU circulation model is to include the inverted barometer effect. The barometric pressure is routinely measured at the major airports, at Thomas Point buoy, and at the CBBT station, which could be used to estimate the pressure field over the Bay. Second, the wind field was taken constant during the assimilation period. However, during frontal passages, the wind speed and direction change quite rapidly, as well as the surface elevation in response to it. An estimate of the wind stress every 3 hours would better represent the temporal changes of the wind field and therefore the wind effect on the circulation in the Bay. These two improvements were beyond the scope of this present study.

5. Summary and Conclusions

The feasibility of dynamical assimilation of tide gauge observations was investigated to estimate the bottom drag coefficient, the surface stress, and the sea level at the Chesapeake Bay mouth, as a first step in improving the modeling of tidal and wind-driven circulation in the Bay. The circulation model used in the study was a two-dimensional vertically integrated shal-

low water model where the bottom stress is defined as a quadratic law with a drag coefficient defined in terms of a Chezy coefficient depending on the total depth of the water column and some roughness. The data assimilation technique was the variational adjoint method where the distance between modeled and observed surface elevations is minimized in order to get the optimal value of the control variables. The adjoint model code was developed from the tangent linear code of the circulation model, and the optimization technique was the limited memory quasi-Newton method [*Gilbert and Lemaréchal*, 1989].

Although the model is simple and does not include stratification, river runoff, or inverted barometer effect, the estimate of bottom friction and of surface stress by assimilating tide gauge observations from 10 permanent stations yields good agreement between modeled and observed surface elevation in the Chesapeake Bay. It is also found that a one-layer model is adequate to model the sea level and the response to the bottom friction and the wind stress in fall. Whether this is true in spring and summer when the stratification is strong requires further investigations.

The assimilation experiments considered in the present study give some insight into the physics of the Chesapeake Bay as well as into empirical quantities such as the bottom drag coefficient. It is found that the drag coefficient displays a fortnightly modulation. Its value for depth < 10 m doubles from spring to neap tide while the variation is much reduced in deeper regions. This fortnightly modulation is altered by the strength of the wind, which, during a frontal passage, yields a drag coefficient value roughly independent of the depth of the water column. It is also found that the response to meteorological forcing is different in the lower and upper Bay. While the estimated wind field in the lower Bay was in excellent agreement with the wind measured at the Chesapeake Bay Bridge Tunnel, the agreement in the upper Bay was not as good. The disagreement between the estimated wind field in the upper Bay and that measured at Thomas Point would indicate that the response of the sea level to the barometric pressure could be at times as important as the response to the wind forcing in the upper Bay.

Acknowledgments.

Y. H. S would like to thank L. M. Lawson, I. M. Navon, and X. Zou for sharing their expertise in data assimilation as well as in adjoint model coding. She also thanks L. P. Atkinson, G. T. Csanady, and A. Valle-Levinson for several stimulating and useful discussions about estuarine modeling. The Management Unit of the Mathematical Models of the North Sea and Scheldt Estuary, especially Georges Pichot and José Ozer, is thanked for allowing the use of their model. S. Gill and Captain C. Fisher of NOAA provided the data and tidal analysis used in this work. Their assistance is greatly appreciated. We thank J. C. Gilbert for supplying the code and documentation for the optimization subroutine, N1QN3. This research was supported by the Center for Coastal Physical Oceanography.

References

Bang, B., Inverse estimation of horizontal pressure gradients and vertical eddy viscosity profiles in shallow waters, Ph.D. thesis, 154 pp., Sch. of Mar. Sci., Coll. of William and Mary, Williamsburg, Va., 1994.

Beckers, P. M., and R. J. Neves, A semi-implicit tidal model of the North European Continental Shelf, *Appl. Math. Modell., 9,* 395-402, 1985.

Blumberg, A., and D. M. Goodrich, Modeling of wind-induced destratification in Chesapeake Bay, *Estuaries, 13,* 236-249, 1990.

Browne, D. R., and C. Fisher, Tide and tidal currents in the Chesapeake Bay, *Tech. Rep. NOS OMA 3,* 84 pp., Natl. Oceanic and Atmos. Admin., Silver Spring, Ma., 1988.

Carrera, J., and S. P. Neumann, Estimation of aquifer parameters under transient and steady state conditions, 1, Maximum likelihood method incorporating prior information, *Water Resour. Res., 22,* 199-210, 1986a.

Carrera, J., and S. P. Neumann, Estimation of aquifer parameters under transient and steady state conditions, 2, Uniqueness, stability, and solution algorithms, *Water Resour. Res., 22,* 211-227, 1986b.

Carrera, J., and S. P. Neumann, Estimation of aquifer parameters under transient and steady state conditions, 3, Application to synthetic and field data, *Water Resour. Res., 22,* 228-241, 1986c.

Courtier, P., and O. Talagrand, Variational assimilation of meteorological observations with the direct and adjoint shallow-water equations, *Tellus,* Ser. A, *42,* 531-549, 1990.

Crean, P. B., T. S. Murty, and J. A. Stronach, *Mathematical Modelling of Tides and Estuarine Circulation: the Coastal Seas of Southern British Columbia and Washington State, Coastal Estuarine Stud.*, vol. 30, edited by M. J. Bowman et al., 471 pp., AGU, Washington, D. C., 1988.

Das, S. K., and R. W. Lardner, On the estimation of parameters of hydraulic models by assimilation of periodic tidal data, *J. Geophys. Res., 96,* 15,187-15,196, 1991.

Das, S. K., and R. W. Lardner, Variational parameter estimation for a two-dimensional numerical tidal model, *Int. J. Numer. Methods Fluids, 15,* 313-327, 1992.

Davies, A. G., Wave interactions with rippled sand beds, in *Physical Oceanography of Coastal and Shelf Seas,* edited by B. Johns, pp. 1-64, Elsevier, New York, 1983.

Fisher, C. W., Tidal circulation in Chesapeake Bay, Ph.D. dissertation, 255 pp., Old Dominion Univ., Norfolk, Va., 1986.

Gilbert J. -C., and C. Lemaréchal, Some numerical experiments with variable-storage quasi-Newton algorithms, *Math. Programming, 45,* 407-435, 1989.

Goodrich, D. M., On stratification and wind-induced mixing in Chesapeake Bay, Ph.D. dissertation, 134 pp., State Univ. of N. Y., Stony Brook, 1985.

Grant, W. D., and O. S. Madsen, Movable bed roughness in oscillatory flow, *J. Geophys. Res., 87,* 469-481, 1982.

Green, M. O., and I. N. McCave, Seabed drag coefficient under tidal currents in the eastern Irish Sea, *J. Geophys. Res., 100,* 16,057-16,069, 1995.

Gross, T. F., and A. R. M. Nowell, Mean flow and turbulence scaling in a tidal boundary flow, *Cont. Shelf Res., 2,* 109-126, 1983.

Haas, L. W., The effect of the spring-neap tidal cycle on the vertical salinity structure of the James, York and Rappahannock Rivers, Virginia, U.S.A., *Estuarine Coastal Mar. Sci., 5,* 485-496, 1977.

Haight, F. J., H. E. Finnegan, and G. L. Anderson, Tides and currents in Chesapeake Bay and tributaries, *Spec. Publ., 162,* 143 pp., U.S. Coast and Geod. Surv., Washington, D. C., 1930.

Hicks, S. D., Tidal wave characteristics of Chesapeake Bay, *Chesapeake Sci., 5,* 103-113, 1964.

Jamart, B. M., and J. Ozer, Some results and comments on the Tidal Flow exercise, *Adv. Water Resour., 12,* 211-220, 1989.

Johns, B., Turbulence modelling beneath waves over beaches, in *Physical Oceanography of Coastal and Shelf Seas,* edited by B. Johns, pp. 111-133, Elsevier, New York, 1983.

Lardner, R. W., A. H. Al-Rabeh, and N. Gunay, Optimal estimation of parameters for a two-dimensional hydrodynamical model of the Arabian Gulf, *J. Geophys. Res., 98,* 18,229-18,242, 1993.

Lawson, L. M., Y. H. Spitz, E. E. Hofmann, and R. B. Long, A data assimilation technique applied to a predator-prey model, *Bull. Math. Biol., 57,* 593-617, 1995.

Lawson, L. M., E. E. Hofmann, and Y. H. Spitz, Time series sampling and data assimilation in a simple marine ecosystem model, *Deep Sea Res., Part II, 43,* 625-651, 1996.

Lewis, J. M., and J. C. Derber, The use of adjoint equations to solve a variational adjustment problem with advective constraints, *Tellus,* Ser. A, *37,* 309-322, 1985.

Li Y., I. M. Navon, P. Courtier, and P. Gauthier, Variational data assimilation with a semi-implicit semi-Lagrangian global shallow-water equations model and its adjoint, *Mon. Weather Rev., 121,* 1759-1769, 1993.

McCave, I. N., Some boundary-layer characteristics of tidal currents bearing sand in suspension, *Mém. Soc. R. Sci. Liège, Collect. 8°, 6,* 187-206, 1973.

Mellor, G. L., and T. Yamada, A hierarchy of turbulence closure models for planetary boundary layers, *J. Atmos. Sci., 31,* 1791-1806, 1974.

Mofjeld, H. O., Depth dependence of bottom stress and quadratic coefficient for barotropic pressure-driven currents, *J. Phys. Oceanogr., 18,* 1658-1669, 1988.

Navon, I. M., X. Zou, J. Derber, and J. Sela, Variational data assimilation with an adiabatic version of the NMC spectral model, *Mon. Weather Rev., 120,* 1433-1446, 1992.

Nocedal, J., Updating quasi-Newton matrices with limited storage, *Math. Comput., 35,* 773-782, 1980.

Officer, C. B., *Physical Oceanography of Estuaries (and Associated Coastal Waters),* 465 pp., John Wiley and Sons, New York, 1976.

Ozer, J., and B. M. Jamart, Tidal motion in the English Channel and southern North Sea: Comparison of various observational and model results, in *Computational Methods in Water Resources,* vol. 1, *Modeling Surface and Subsurface Flows,* edited by M. A. Celia et al., pp. 267-273, Elsevier, New York, 1988.

Ozer, J., E. Deleersnijder, and B. M. Jamart, Model intercomparison: Description of a semi-implicit numerical model for shallow-water wave equations, MUMM's contribution to MAST-0050-C (SMA), *Tech. Rep. 1,* MUMM, Brussels, 1990.

Panchang, V. G., and J. J. O'Brien, On the determination of hydraulic model parameters using the adjoint state formulation, in *Modelling in Marine Systems,* edited by A. M. Davies, pp. 6-18, CRC Press, Boca Raton, Fla., 1989.

Paraso, M. C., and A. Valle-Levinson, Meteorological influences on sea level and water temperature in the lower Chesapeake Bay: 1992, *Estuaries, 19,* 548-561, 1996.

Richardson, J. E., and V. G. Panchang, A modified adjoint method for inverse eddy viscosity estimation in coastal circulation models, *Estuarine and Coastal Modeling, Proceedings of the 2nd International Conference,* edited by M. L. Spaulding, pp. 733-745, ASCE, New York, N. Y., 1992.

Ronday, F., *Modèles Hydrodynamiques,* vol. 3, *Modélisation des systèmes marins, Projet Mer, Rapport Final,* 270 pp., Serv. du Premier Minist., Programmation de la Polit. Sci., Bruxelles, 1976.

Sasaki, Y., Some basic formalisms in numerical variational analysis, *Mon. Weather Rev., 98,* 875-883, 1970.

Schwab, D. J., An inverse method for estimating wind stress from water-level fluctuations, *Dyn. Atmos. Oceans, 6,* 251-278, 1982.

Seiler, U., Estimation of open boundary conditions with the adjoint method, *J. Geophys. Res., 98,* 22,855-22,870, 1993.

Smedstad, O. M., and J. J. O'Brien, Variational data assimilation and parameter estimation in an equatorial Pacific ocean model, *Prog. Oceanogr., 26,* 179-241, 1991.

Spitz, Y. H., A feasibility study of dynamical assimilation of tide gauge data in the Chesapeake Bay, Ph.D. dissertation, 167 pp., Old Dominion Univ., Norfolk, Va., 1995.

Spitz, Y. H., J. R. Moisan, M. R. Abbott, and J. G. Richman, Data assimilation and a pelagic ecosystem model: parameterization using time series observations, *J. Mar. Syst.,* in press, 1998.

Swanson, R. L., Variability of tidal datums and accuracy in determining datums from short series of observations, *NOAA Tech. Rep. NOS, 64,* 41 pp., 1974.

Talagrand, O., The use of adjoint equations in numerical modeling of the atmospheric circulation, in *SIAM , Automatic Differentiation: Theory, Implementation, and Application,* edited by A. Griewanek and G. Corliss, pp. 169-180, Soc. for Ind. and Appl. Math., Philadelphia, Pa., 1991.

Talagrand, O., and P. Courtier, Variational assimilation of meteorological observations with the adjoint vorticity equation, I, Theory, *Q. J. R. Meteorol. Soc., 113,* 1311-1328, 1987.

Taylor, P. A., and K. R. Dyer, Theoretical models of flow near the bed and their implication for sediment transport, in *The Sea,* vol. 6, *Marine Modelling,* edited by E. D. Goldberg et al., pp. 579-601, Wiley-Interscience, New York, 1977.

Thacker, W. C., Fitting models to inadequate data by enforcing spatial and temporal smoothness, *J. Geophys. Res., 93,* 10,655-10,665, 1988.

Thacker, W. C., and R. B. Long, Fitting dynamics to data, *J. Geophys. Res., 93,* 1227-1240, 1988.

Ullman, D. S., and R. E. Wilson, Model parameter estimation from data assimilation modeling: Temporal and spatial variability of the bottom drag coefficient, *J. Geophys. Res., 103,* 5531-5549, 1998.

Valle-Levinson, A., Observation of barotropic and baroclinic exchanges in the lower Chesapeake Bay, *Cont. Shelf Res., 15,* 1631-1647, 1995.

Vieira, M., The meteorologically driven circulation in mid-Chesapeake Bay, *J. Mar. Res., 44,* 473-493, 1986.

Wang, D. -P., Subtidal sea level variations in the Chesapeake Bay and relations to atmospheric forcing, *J. Phys. Oceanogr., 9,* 413-421, 1979a.

Wang, D. -P., Wind-driven circulation in the Chesapeake Bay, winter 1975, *J. Phys. Oceanogr., 9,* 564-572, 1979b.

Wang, D. -P., and A. Elliott, Non-tidal variability in the Chesapeake Bay and Potomac River: Evidence for non-local forcing, *J. Phys. Oceanogr., 8,* 225-232, 1978.

Werner, F. E., and D. R. Lynch, Field verification of wave equation tidal dynamics in the English Channel and southern North Sea, *Adv. Water Resour., 10,* 115-130, 1987.

Wong, K. -C., and R. Garvine, Observations of subtidal, wind-induced variability in the Delaware estuary, *J. Geophys. Res., 89,* 10,589-10,597, 1984.

Wright, L. D., Benthic boundary layers of estuarine and coastal environments, *Rev. Aquat. Sci., 1,* 75-95, 1989.

Wright, L. D., D. B. Prior, C. H. Hobbs, R. J. Byrne, J. D. Boon, L. C. Schaffner, and M. O. Green, Spatial variability of bottom types in the lower Chesapeake Bay and adjoining estuaries and inner shelf, *Estuarine Coastal Shelf Sci., 24,* 765-784, 1987.

Wright, L. D., J. D. Boon, J. P. Xu, and S. C. Kim, The bottom boundary layer of the bay stem plains environment of lower Chesapeake Bay, *Estuarine Coastal Shelf Sc., 35,* 17-36, 1992.

Yu, L., and J. J. O'Brien, Variational estimation of the wind stress drag coefficient and the oceanic eddy viscosity profile, *J. Phys. Oceanogr., 21,* 709-719, 1991.

Zou, X., I. M. Navon, and F. X. Le Dimet, Incomplete observations and control of gravity waves in variational data assimilation, *Tellus, Ser. A, 44,* 273-296, 1992a.

Zou, X., I. M. Navon, and F. X. Le Dimet, An optimal nudging data assimilation scheme using parameter estimation, *Q. J. R. Meteorol. Soc., 118,* 1163-1186, 1992b.

Zou, X., A. Barcilon, I. M. Navon, J. Whitaker, and D. G. Cacuci, An adjoint sensitivity study of blocking in a two-layer isentropic model, *Mon. Weather Rev., 12,* 2833-2857, 1993.

J. M. Klinck, Center for Coastal Physical Oceanography, Old Dominion University, Norfolk, VA 23529. (e-mail klinck@ccpo.odu.edu)

Y. H. Spitz, College of Oceanic and Atmospheric Sciences, Oregon State University, Corvallis, OR 97331. (e-mail yvette@oce.orst.edu)

(Received May 21, 1997; revised November 20, 1997; accepted January 27, 1998.)